Accepted Manuscript

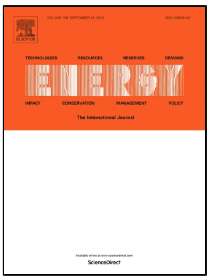

Optimization with a simulated annealing algorithm of a hybrid system for renewable energy including battery and hydrogen storage

Weiping Zhang, Akbar Maleki, Marc A. Rosen, Jingqing Liu

PII:	S0360-5442(18)31648-7
DOI:	10.1016/j.energy.2018.08.112
Reference:	EGY 13588
To appear in:	*Energy*
Received Date:	09 March 2018
Accepted Date:	14 August 2018

Please cite this article as: Weiping Zhang, Akbar Maleki, Marc A. Rosen, Jingqing Liu, Optimization with a simulated annealing algorithm of a hybrid system for renewable energy including battery and hydrogen storage, *Energy* (2018), doi: 10.1016/j.energy.2018.08.112

Optimization with a simulated annealing algorithm of a hybrid system for renewable energy including battery and hydrogen storage

Weiping Zhang[1,2], Akbar Maleki*[3], Marc A. Rosen[4], Jingqing Liu[5]

[1]Department of Electronic Information Engineering, Nanchang University, Nanchang, China

[2]Industry Technology Research Institute, Zhejiang University, Tianjian, China

[3]Department of Renewable Energies, Faculty of New Science & Technologies, University of Tehran, Tehran, Iran

[4]Faculty of Engineering and Applied Science, University of Ontario Institute of Technology, Oshawa, Ontario, L1H 7K4, Canada

[5]College of Civil Engineering and Architecture, Zhejiang University, Hangzhou, China.

Abstract

Wind and solar energy based hybrid systems incorporating energy storage can often provide cost effective and reliable energy alternatives to the conventional systems commonly used by remote consumers. To integrate a high level of variable wind and solar energy, energy storage is important. The primary contribution made by the present article is the development of a new efficient methodology for modeling and optimally sizing a hybrid system for renewable energy considering two energy storage devices: hydrogen (as a form of chemical storage) and batteries (as a form of electrochemical storage). To optimize the decision variable values, modified versions of the simulated annealing algorithm-based chaotic search and harmony search are developed. This is dedicated to the optimization of the supply of

* Corresponding Author.
E-mail addresses: akbar.maleki20@yahoo.com, a_maleki@ut.ac.ir (A. Maleki).

residential electrical load via stand-alone hybrid energy systems, so as to achieve the minimum life cycle cost of the system by continuous and integer decision variables. The proposed modified approach is used to size optimally the components of six schemes for a remote area in Iran: wind/hydrogen, solar/hydrogen, solar/wind/hydrogen, wind/battery, solar/battery, and solar/wind/battery. To determine the methodology quality, the performance of the proposed hybrid algorithm is contrasted with that for simulated annealing and hybrid harmony search and simulated annealing algorithms. The optimization results demonstrate that a wind and solar energy based hybrid system with electrochemical storage offers more cost effective and reliable energy than a hybrid system for renewable energy with chemical storage. Also, among hybrid systems, the wind/battery system is clearly advantageous economically for supplying power. The portions of life cycle cost of the wind turbine, batteries, and converter/inverter are 67%, 5%, and 28%, respectively. The relative errors between the Mean index of are shown to be at most 11%. Finally, a comparison of the Min., Max., Mean, and Std. values, in the six hybrid systems, shows that the proposed hybrid algorithm is more robust than the others considered since it has lower index values.

Keywords: Energy storage; Hybrid energy system; Renewable energy; Optimal design; Simulated annealing.

Nomenclature

A_{PV}	photovoltaic (PV) surface area (m^2)	N_{H2}	number of hydrogen tanks
A_{WT}	area of wind turbine blades (m^2)	N_{BAT}	number of batteries
$bw_{\min}$	minimum bandwidth	N_d	number of decision variables
bw	bandwidth of generation	p_{PV}	output power of each PV system (kW)
$bw_{\max}$	maximum bandwidth	P_{PV}	output electrical power of PV panels (kW)
C_B	nominal capacity of battery bank (kWh)	PW_{FC}	present worth fuel cell ($)
CC	capital cost ($)	P_r	rated power of the wind turbine (kW)
CRF	capital recovery factor	p_{WT}	produced power of each wind turbine (kW)
C_{PV}	unit cost of PV panel ($/$m^2$)	P_{WT}	output electrical power of wind turbines (kW)
$C_{Mnt\text{-}PV}$	annual operation and maintenance cost of PV system ($/$m^2$/year)	$PAR_{\min}$	minimum pitch adjusting rate
$C_{Mnt\text{-}WT}$	annual operation and maintenance cost of wind turbine ($/$m^2$/year)	$PAR_{\max}$	maximum pitch adjusting rate
C_{WT}	unit cost of wind turbine ($/$m^2$)	PAR	pitch adjusting rate
$C_{Mnt\text{-}FC}$	annual maintenance cost of each fuel	r, r_1, r_2	uniform random number in the range [0, 1]

	cell ($/year)	and r_3	
C_{FC}	fuel cell cost ($)	R	solar radiation (kW/m^2)
C_{Elect}	Electrolyzer cost ($)	RC	replacement cost ($)
$C_{Mtn\text{-}Elec}$	annual maintenance cost of electrolyzer ($/year)	SOC	state of the charge
C_{H2}	storage tank cost ($)	s	step size
$C_{Mnt\text{-}H2}$	annual maintenance cost of hydrogen tank ($/year)	T	temperature
$C_{Conv/Inv}$	converter/inverter cost ($)	T_0	starting temperature
C_{BS}	battery price ($)	v	wind speed (m/s)
DOD	maximum depth of discharge	v_r	rated speed of the wind generator (m/s)
E_{PV}	the electrical energy generated of PV panels (kWh)	$v_{cut\text{-}in}$	cut-in speed of the wind generator (m/s)
E_{WT}	electrical energy generated of wind turbines (kWh)	$v_{cut\text{-}out}$	cut-out speed of the wind generator (m/s)
E_L	energy demand (kWh)	WF	a vector having elements randomly distributed in the range [-*wf, wf*]
E_g	generated energies by the PV panels and wind turbines (kWh)	X_{FC}	number of times a replacement of a fuel cell
$HMCR$	harmony memory considering rate	$x(iter)$	current solution
$iter$	iteration index	x_{new}	new solution
$iter_{\max}$	maximum number of iterations	η_{PV}	combined efficiency of PV collectors and the DC/DC converter (%)
j	interest rate (%)	η_{FC}	FC efficiency (%)
LCC	life cycle cost ($)	η_{inv}	inverter efficiency (%)
L_{FC}	fuel cell lifetime (year)	η_{Elect}	electrolyzer efficiency (%)
MC	maintenance cost ($)	η_{BC}	battery bank charging efficiency (%)
n	life span of the system (years)	η_{BD}	discharging efficiency of battery bank (%)
N_{PV}	number of PV panel	σ	hourly self-discharge rate
N_{WT}	number of wind turbine		

1. Introduction

Preventing environmental impact and conserving fossil fuels for future generations are two important reasons for using sources of renewable energy, especially wind turbines (WT) and solar photovoltaics (PV) [1]. Increasing penetration of systems for renewable energy will likely decrease electricity generation costs and electricity grid reliability, largely due to renewable energy variability and the lack of large-scale economical storage capabilities. Currently there are still about 1.2 billion people in the world without grid electricity, most of them living in remote areas [2]. Due to their low emissions and low maintenance costs, renewable energy systems are increasingly being used at present to provide electrical power to various locations, especially rural, which produce electrical power independent of the utility grid, sometimes because grid connection is not available. Owing to seasonal and periodical

variations, using more than one power source to supply a user can enhance energy security and reliability over systems having only one renewable energy system. Hybrid systems for renewable energy based on photovoltaics and wind turbines are well known and reliable and have long lifetimes [3]. The main advantages of wind and solar energy are low greenhouse gas emissions and, in some instances, advantageous economics.

Energy storage for hybrid solar/wind systems is important as a consequence of the intermittency of wind and solar energy. For storage of electrical energy, lead acid batteries using deep cycles often are used, even though environmental concerns related to their use can restrict utilization of hybrid solar/wind/battery systems. This has led to research into alternative energy storage methods [3].

One alternative for energy storage is the use of fuel cells (FCs) with hydrogen production electrolyzers and hydrogen storage tanks. Solar/wind/hydrogen energy systems can provide clean and reliable energy with lower maintenance costs. In such systems, electrolyzers utilize excess electricity from wind and solar energy systems to produce hydrogen, which can be utilized in a fuel cell to provide electricity for periods of high electrical demand.

Optimal design is important for reliability and cost effectiveness. Oversizing can lead to high initial costs and other challenges, while under sizing can lead to operational limitations and energy shortfalls, despite lower initial costs. But, optimizing hybrid renewable energy systems with energy storage can reduce initial costs and raise efficiencies, while allowing for various energy resources. Therefore, optimization is particularly important for the accurate and effective evaluation of optimal designs of hybrid energy systems. In this regard, hybrid systems for renewable energy including hydrogen and battery energy storage have received much attention recently. Past articles are cited according to these features in Table 1. The studies listed in Table 1 suggest that hybrid energy systems, specifically solar and wind energy based ones, are advantageous for supplying the load of remote areas, to avoid the limitation of one energy system. Also, HOMER software, a commonly used tool, is used for optimizing, designing and performance evaluation of a hybrid solar/wind system. However, HOMER software has

some limitations, like black box coding, different working platforms, and inflexibility regarding optimization techniques. In this regard, artificial intelligence techniques have the potential to improve the process of optimization. Finally, hybrid optimization methodologies are recommended for hybrid system research to avoid the limitation of one methodology.

Table 1: Summary of the literature review.

Authors/year	Solar	Wind	Battery	Diesel	Hydrogen	Other	Method
Ekren [4]/2010	✓	✓	✓	-	-	-	Simulated annealing
Calderón et al. [5]/2010	✓	✓	-	-	✓	-	Simulation
Khatib et al. [6]/2011	✓	-	-	✓	-	-	Simulation
Dufo-López et al. [7]/2011	✓	✓	✓	✓	-	-	Pareto evolutionary algorithm
Belfkira et al. [8]/2011	✓	✓	✓/-	✓	-	-	Simulation
Raj and Ghosh [9]/2012	✓	-	-	✓/-	✓/-	-	Simulation
Valdés et al. [10]/2012	✓	-	-	-	✓	-	Experimental/simulation
Merei et al. [11]/2013	✓	✓	✓	✓	-	-	Genetic algorithm (GA)
Castañeda et al. [12] /2013	✓	-	✓	-	✓	-	Simulation MATLAB
Hiendro et al. [13]/2013	✓	✓	✓	-	-	-	HOMER software
Rekioua et al. [14]/2014	✓	-	-	-	✓	-	Simulation
Maleki and Askarzadeh [15]/2014	✓	✓	✓	✓	-	-	Harmony search
Bensmail et al. [16]/2015	✓	-	-	-	✓	-	Simulation
Tsuanyo et al.[17]/2015	✓	-	-	-	✓	-	HOMER software
Chauhan and Saini [18]/2016	✓	✓	-	-	-	✓	Harmony search
Shankar and Mukherjee [19]/2016	✓	✓	-	-	-	✓	Harmony search
Halabi et al.[20]/2017	✓	-	✓	✓	-	-	HOMER software
Nadjemi et al. [21]/2017	✓	✓	✓	-	-	-	Cuckoo search
Hatata et al. [22]/2018	✓	✓	✓	-	-	-	GA
Ahmad et al. [23]/2018	✓	✓	-	-	-	✓	HOMER software
Guangqian et al. [24]/2018	✓	✓	✓	-	-	✓	Simulated annealing
Peng et al. [25]/2018	✓	✓	✓	-	-	-	Simulation; optimization program
Eteiba et al.	✓	-	-	-	-	✓	Harmony search

[26]/2018							
Khiareddine et al. [27]/2018	✓	✓	✓	-	✓	-	Simulation; energy management strategy

71 Belfkira et al. [8], for instance, developed a method for optimally sizing a hybrid system for
72 wind/solar/diesel energy that operates on a stand-alone basis. They also investigated the impact of
73 battery energy storage on the system's total cost. Koutroulis et al. [28] describe a procedure for
74 optimally sizing systems for wind/solar energy, in which the objective function is minimized using a
75 genetic algorithm. Ismail et al. [29] techno-economically assessed and designed a hybrid energy system

using diesel-PV-battery technology, while Chong et al. [30] techno-economically analyzed an innovative hybrid system for wind-solar energy. Tzamalis et al. [31] techno-economically compared the energy cost using either hydrogen technology or a diesel generator, considering various cases that were analyzed to select the optimal one. Karakoulidis et al. [32] modeled a hybrid system for PV/diesel/battery energy that satisfies a known electric demand. Kaabeche et al. [33] developed an iterative procedure to optimally size components of a hybrid system for solar/wind/battery energy. An iterative optimization methodology was developed by Kaabeche and Ibtiouen [34] based on energy cost, total energy deficit and total net present cost. Caballero et al. [35] proposed a methodology using life cycle cost for optimally designing a grid-connected, small system for renewable energy, while Rajanna and Saini [36] used a genetic algorithm for optimizing an integrated system for renewable energy, considering four regions in Karnataka, India, utilizing various sources of renewable energy with energy storage via batteries. Fathy [37] used a mine blast algorithm for the optimization for Helwan, Egypt of a hybrid system for renewable energy, by minimizing cost. Hassan et al. [38] developed a modified routine with particle swarm optimization to determine the optimum combination of both a grid connected solar/wind system and a solar/wind/battery system that operates on a stand-alone basis. Suhane et al. [39] applied ant colony optimization for optimizing the mix of a wind/solar/battery system by minimizing total annual cost for a village in India.

Despite the fact that various studies have been performed of facets of hybrid systems for renewable energy, there has not been a report of an informative model-based effective storage system and an efficient tool for optimizing system sizing.

An efficient optimization technique is needed for hybrid systems for renewable energy because their optimal sizing constitutes an optimization problem that includes continuous and integer decision variables, and is both non-linear and non-convex. Deterministic approaches normally require gradient information, are sensitive to the initial point and cannot manage the size of the optimization problem. Nevertheless, some optimization methods for optimization of hybrid systems have been reported,

including HOMER [40], genetic algorithm (GA) [41], particle swarm optimization (PSO) [42], mine blast algorithm [37], simulated annealing (SA) [43], cuckoo search algorithm [21], biogeography based optimization [44], Big Bang–Big Crunch algorithm [45], and harmony search (HS) [18]. Heuristic techniques have attracted attention as they provide a viable alternative by integrating random search and nature-inspired phenomenon. However, new heuristic techniques are found to be more acceptable than traditional heuristic techniques [46]. Nevertheless, there are few studies that are performed to ascertain the optimal parameters of hybrid energy system using hybrid optimization algorithm. Consequently in this study heuristic methods are used for optimization, because of their ability to search global and local optima, fast convergence and good calculation accuracy.

Harmony search (HS) and simulated annealing (SA) algorithms have been introduced recently as effective optimization techniques to deal with the optimal solution of problems. Furthermore, numerous uses of the simulated annealing algorithm for various systems have been reported, including: energy management [47], planning the location and rating of distributed energy storage [48], handling the energy of electric vehicles [49], and energy management in microgrids [50]. Also, numerous uses of the harmony search algorithm for various systems have been reported, which demonstrate its superiority including: optimal planning [51], network partitioning [52], charge scheduling of an energy storage system [53], improving exploration and exploitation capabilities [54]. This paper, therefore, proposes a harmony search and a simulated annealing based model to solve the optimization problem. This exploits the fact that harmony search and simulated annealing have the advantages of good convergence speed [53], flexibility and good efficiency [55] when compared to classical techniques [56].

The primary objective of the research reported here is to construct a framework for optimally sizing of hybrid systems for renewable energy that incorporate hydrogen and battery energy storage devices. This is done by determining the area occupied by PV panels, the cross sectional area swept by the blades of the wind turbine and the energy storage capacity (battery bank and hydrogen storage tanks). This is accomplished via a modified hybrid optimization algorithm-based simulated annealing. The hybrid

chaotic search/harmony search/simulated annealing (HCHSA) algorithm includes harmony search, chaotic search, and simulated annealing. The optimization algorithm minimizes the hybrid system life cycle cost by varying decision variables.

To support global optimization, a hybrid generic probabilistic algorithm utilizing simulated annealing, chaotic search, and harmony search is employed. The algorithm is a conceptually simple and efficient search method, which is easy to implement, requires only one initial solution and can escape local optima via probabilistic mechanisms. Results of HCHSA algorithm have been compared with those from simulated annealing [57], hybrid harmony search and simulated annealing algorithms [58].

This paper extends the work reported in the literature significantly, by presenting several important innovations. More important, to help address the complexity of the optimization of hybrid energy schemes, hybrid heuristic methods are proposed in this paper including chaotic search, harmony search, and simulated annealing algorithms. The models are dedicated to the optimization of the supply of residential electrical load via stand-alone hybrid energy systems, so as to achieve the minimum cost of the overall system, contrary to existing approaches, which only rely on a simplistic model of the heuristic methods. Also, formulating and solving optimally the sizing for a hybrid energy system which integrates wind and solar energy sources with two storages, including chemical storage via hydrogen and electrochemical storage via batteries, is considered with four decision variables. This contrasts with existing approaches that only consider one or two of these sources for simplicity. Moreover, the proposed modified approach is used to size optimally the components of six schemes, contrary to existing systems which only consider one of these systems for simplicity. The optimization process is implemented and tested by using actual data for a remote region of Kerman, Iran. Finally, original simulated annealing and hybrid harmony search and simulated annealing algorithms are applied to solve the problem to permit the results to be compared with those obtained by the proposed hybrid algorithm. Consequently, the article provides a comprehensive modeling and an efficient optimization algorithm for stand-alone hybrid energy schemes. This presentation of the study includes the following parts. The

optimization framework is described in Section 2, while the simulated annealing algorithm, hybrid harmony search and simulated annealing algorithm, and HCHSA algorithm are explained in section 3. Section 4 provides simulation results and Section 5 concluding remarks.

2. Optimization framework

A schematic is shown in Fig. 1 of the proposed system for renewable energy. Prior to the optimization, an energy balance is obtained, hourly throughout the year. This involves determining the quantity of energy produced with each resource and necessitates modeling all components of the system. The optimization framework, including component modelling, is described in this section.

Fig. 1

2.1. Modeling of system components

The optimization of a hybrid energy system requires the mathematical modeling of each component of the system. In the following subsections, modeling of the components and the optimization framework are described in detail.

2.1.1. Electrical power from PV array

The electrical power p_{PV} generated by a PV array comprised of a set of collectors at time t can be written as follows [59]:

$$p_{PV}(t) = R(t) \times A \times \eta_{PV} \tag{1}$$

where A denotes PV area in m^2, η_{PV} combined efficiency of PV collectors and the DC/DC converter, and R the incident solar radiation in kW/m^2. The overall power produced can be expressed as $P_{PV}(t) = N_{PV} \times p_{PV}(t)$ and the electrical energy generated in one hour as $E_{PV}(t) = P_{PV}(t) \cdot dt$, where N_{PV} denotes number of PV systems and dt time step.

2.1.2. Power produced by wind turbine

A WT starts to generate electricity if the speed of the wind exceeds a cut-in value and, for protection, stops operating if the speed of the wind surpasses a cut-out value [60]. Hence, the power generation by the wind turbine P_{WT} is constant when the speed

175 of the wind lies between these extremes and can be expressed as follows:

$$p_{WT}(t)=\begin{cases}0 & v(t)\le v_{cut-in} \quad or \quad v(t)\ge v_{cut-out}\\ P_r\dfrac{v(t)-v_{cut-in}}{v_r-v_{cut-out}} & v_{cut-in}<v(t)<v_r\\ P_r & v_r<v(t)<v_{cut-out}\end{cases} \tag{2}$$

176 Here, P_r denotes the rated power of the wind turbine in kW and v the speed of the wind in m/s, while
177 v_r, $v_{cut\text{-}out}$ and $v_{cut\text{-}in}$ respectively denote the rated, cut-out and cut-in speeds in m/s for the wind turbine.
178 For N_{WT} wind generators, the power produced is expressible as $P_{WT}(t)=N_{WT}\times p_{WT}(t)$ and the
179 electrical energy generated in one hour as $E_{WT}(t)=P_{WT}(t)\cdot dt$.

180 2.1.3. Storage system

181 The two kinds of energy storage commonly utilized in hybrid energy systems are hydrogen storage units
182 (with an electrolyzer and fuel cell (FC)) and batteries of the lead-acid type. Appropriate capacities of the
183 hydrogen storage tank and battery bank depend on the state of charge (SOC) of each. The energy
184 generation rate at time *t* by the WTs and PV panels is expressible as:

$$E_g(t)=E_{WT}(t)+E_{PV}(t) \tag{3}$$

185 Depending on the load E_L, E_g may or may not be adequate at a specific time for providing the power
186 required. For charging and discharging of the storages, the SOC is described below.

187 **Hydrogen storage:**

188 For determining the storage system efficiency in this article, the electrolyzer charging efficiency and the
189 FC discharging efficiency are utilized. If $E_g(t)\ge\dfrac{E_L(t)}{\eta_{inv}}$, the electrolyzer charges the hydrogen tanks,
190 with the quantity of hydrogen stored given by [59].

$$SOC_{HT}(t)=SOC_{HT}(t-1)+\left[E_g(t)-\frac{E_L(t)}{\eta_{inv}}\right]\cdot\eta_{Elect} \tag{4}$$

191 The FC supplies the electrical load if $E_g(t) \le \frac{E_L(t)}{\eta_{inv}}$, with the quantity of hydrogen stored at hour t is

192 given by [59]:

$$SOC_{HT}(t) = SOC_{HT}(t-1) - \left[\frac{E_L(t)}{\eta_{inv}} - E_g(t)\right] / \eta_{Elect} \quad (5)$$

193 Here, η_{FC} denotes the FC efficiency, η_{inv} the inverter efficiency and η_{Elect} the electrolyzer efficiency.

194 **Battery storage:**

195 When $E_g(t) \ge \frac{E_L(t)}{\eta_{inv}}$, the batteries store surplus electricity. For the battery bank, the SOC can be given

196 as [61]:

$$SOC_{BS}(t) = SOC_{BS}(t-1) \cdot (1-\sigma) + \left[E_g(t) - \frac{E_L(t)}{\eta_{inv}}\right] \cdot \eta_{BC} \quad (6)$$

197 where η_{BC} denotes the battery bank charging efficiency and σ the self-discharge rate on an hourly basis.

198 As the maximum energy storage in batteries during optimization cannot surpass the state of charge

199 maximum, $SOC_{BS\text{-}max}$,

$$SOC_{BS}(t) < SOC_{BS-\max} \quad (7)$$

200 where $SOC_{BS\text{-}max}$ denotes the nominal battery bank capacity C_B. If $E_g(t) \le \frac{E_L(t)}{\eta_{inv}}$, then the load is

201 provided by the storage. The battery bank SOC can be expressed as [61]:

$$SOC_{BS}(t) = SOC_{BS}(t-1) \cdot (1-\sigma) - \left[\frac{E_L(t)}{\eta_{inv}} - E_g(t)\right] / \eta_{BD} \quad (8)$$

202 where η_{BD} denotes for the battery bank the discharging efficiency.

203 Note that SOC_{BS} should exceed the state of charge minimum $SOC_{BS\text{-}min}$ so as to elongate the life of the

204 batteries, as per the following constraint [62]:

$$SOC_{BS}(t) \ge SOC_{BS-\min} \quad (9)$$

206 where the maximum depth of discharge (DOD) determines $SOC_{BS\text{-}min}$ as follows:

$$SOC_{BS-\min} = (1 - DOD) \cdot C_B \quad (10)$$

2.2. Life cycle costing

The life cycle cost (LCC) is utilized here for the cost analysis of the system for renewable energy. LCC is expressible as:

$$LCC = CC + MC + RC \quad (11)$$

where CC, MC and RC denote cost for capital, operation and maintenance, and replacement. In this study, all monetary units are in US dollars.

2.2.1. Life cycle cost of PV collectors

The life cycle cost of a PV collector (LCC_{PV}) can be written as its capital cost (CC_{PV}) plus operation and maintenance cost (MC_{PV}). That is,

$$LCC_{PV} = CC_{PV} + MC_{PV} \quad (12)$$

where

$$CC_{PV} = CRF \cdot A_{PV} C_{PV} \quad (13)$$

$$MC_{PV} = A_{PV} C_{Mnt-PV} \quad (14)$$

$$CRF(j, n) = \frac{j(1+j)^n}{(1+j)^n - 1} \quad (15)$$

and where C_{PV} denotes PV collector unit cost, $C_{Mnt\text{-}PV}$ annual maintenance cost of each PV panel, CRF capital recovery factor, n life span and j interest rate.

Presuming the project lifetime n equals the lifetime of the PV panel, its replacement cost is nil (i.e., RC_{PV}=0).

2.2.2. Life cycle cost of wind turbine

The life cycle cost for a wind turbine (LCC_{WT}) can be written as its capital cost (CC_{WT}) plus operation and maintenance cost (MC_{WT}). That is,

$$LCC_{WT} = CC_{WT} + MC_{WT} \quad (16)$$

where

$$CC_{WT} = CRF \cdot A_{WT} C_{WT} \quad (17)$$

$$MC_{WT} = A_{WT} C_{Mnt-WT} \quad (18)$$

and where $C_{Mnt\text{-}WT}$ the annual maintenance cost per WT and C_{WT} denotes the unit cost for the WTs. Again, presuming the project lifetime equals the wind turbine lifetime, its replacement cost is zero (RC_{WT}=0).

2.2.3. Life cycle cost of storage system

The wind turbine and PV panel lifetimes, considered to be n here, exceed the fuel cell lifetime L_{FC}. Thus, additional expenditures are required before the project end. The number of times a replacement of a fuel cell is needed for the horizon of n years can be expressed as $X_{FC} = \frac{n}{L_{FC}} - 1$.

Since the fuel cell lifetime is taken to be 5 years and the project life 20 years [1] in this study, the fuel cell is replaced three times during the project life. The fuel cell life cycle cost can be written as its capital cost (CC_{FC}) plus operation and maintenance cost (MC_{FC}):

$$LCC_{FC} = CC_{FC} + MC_{FC} \tag{19}$$

where

$$CC_{FC} = PW_{FC} \cdot CRF \tag{20}$$

$$PW_{FC} = C_{FC} \sum_{k=0,5,10,15} \frac{1}{(1+j)^k} \tag{21}$$

$$MC_{FC} = C_{Mnt-FC} \cdot N_{FC} \tag{22}$$

and where PW_{FC} denotes fuel cell present worth, $C_{Mnt\text{-}FC}$ annual maintenance cost of each fuel cell and C_{FC} fuel cell cost. The life cycle cost of electrolyzer is determined as for the FC, noting that the fuel cell lifetime is presumed here to be five years [63].

Similarly, the combination of capital cost (CC_{H2}) and operation and maintenance cost (MC_{H2}) permits the life cycle cost for the hydrogen storage tank (LCC_{H2}) to be expressed:

$$LCC_{H2} = CC_{H2} + MC_{H2} \tag{23}$$

where

$$CC_{H2} = N_{H2} \cdot C_{H2} \cdot CRF \tag{24}$$

$$MC_{H2} = C_{Mnt-H2} \cdot N_{H2} \tag{25}$$

and where N_{H2} denotes number of hydrogen storage tanks, C_{H2} unit cost per storage tank, and $C_{Mnt\text{-}H2}$ annual maintenance cost per hydrogen tank.

Presuming lifetimes of the hydrogen storage tanks and project are equal, the replacement cost is zero for the hydrogen storage tanks (RC_{H2}=0). The battery bank life cycle cost is obtained as for the FC.

2.3. Objective function and constraints

For the renewable energy system, the optimization objective is to minimize, subject to relevant constraints, total system cost. The fitness function can be written as:

$$Minimize\ TLCC(A_{PV}, A_{WT}, N_{H2}, N_{BAT}) = Min. \sum_{m=PV,WT,FC,Ele,H2,BAT,Inv} LCC_m \quad (26)$$

In the sizing problem, the decision variables are as follows: PV surface area (A_{PV}), area of wind turbine blades (A_{WT}), number of batteries (N_{BAT}) and number of hydrogen tanks (N_{H2}). Additionally, the following constraints are satisfied:

$$0 \le A_{PV} \le A_{PV-Max} \quad (27)$$

$$0 \le A_{WT} \le A_{WT-Max} \quad (28)$$

$$0 \le N_{H2} \le N_{H2-Max} \quad (29)$$

$$0 \le N_{BAT} \le N_{BAT-Max} \quad (30)$$

The four decision variables in this problem are optimally adjusted where A_{WT} and A_{PV} are continuous decision variables and N_{H2}, and N_{BAT} is an integer decision variable.

3. Optimization algorithm-based simulated annealing

In this section, a hybrid chaotic search/harmony search/simulated annealing (HCHSA) algorithm is proposed for optimization of hybrid renewable energy systems. Firstly, an introduction to simulated annealing (SA) and hybrid harmony search and simulated annealing (HS-SA) algorithms is provided. Then, the proposed HCHSA method is described.

Simulated annealing algorithm

Simulated annealing (SA) is an iterative meta-heuristic for solving non-convex and nonlinear optimization problems. SA stems from metallurgical annealing, in which controlled heating and cooling lowers defects and increases crystal size in a metal. Consequently, a search with SA begins with a temperature T sufficiently large to permit a search of a wide area and ends with a temperature sufficiently small so as to follow the steepest descent heuristic in moving downhill. As the iterations

move forward in SA, the temperature slowly is reduced [61]. The SA method used here is that proposed in [57] as discrete SA.

The solution at an iteration (*iter*) is *x*(*iter*), while *f*(*x*(*iter*)) denotes the corresponding objective function. The likelihood that the subsequent solution *x*(*iter* + 1) is found at a random solution proximate to *x*(*iter*), x_{new}, is a function of the difference among the relevant fitness values, $\Delta F = f\left(x_{new}\right) - f\left(x\left(iter\right)\right)$ and the temperature. So, the subsequent solution is at:

$$x\left(iter+1\right) = \begin{cases} x_{new} & if \ \exp(-\Delta F / T) > r \\ x\left(iter\right) & o.w. \end{cases} \tag{31}$$

Here, *r* denotes a uniform random number in the range [0, 1].

If $\Delta F \le 0$, the parameter x_{new} is accepted always. The possibility of opting for x_{new} as *x*(*iter* + 1) despite the value of the function being better at *x*(*iter*) than x_{new}, depending on the values of ΔF and *T*. New solutions continue to be produced up to the maximum number of iterations, $iter_{max}$. With SA, x_{new} and *T* vary during the iterations in the following manners:

$$x_{new} = x\left(iter\right) + WF \tag{32}$$

$$T\left(iter+1\right) = s \times T\left(iter\right) \tag{33}$$

Here, *s* denotes step size and *WF* a vector having elements randomly distributed in the range [-*wf*, *wf*]. A starting temperature T_0 is used to commence the algorithm.

Hybrid chaotic search/harmony search/simulated annealing algorithm

Harmony search is a powerful metaheuristic method with excellent exploitation capabilities, however it has a very serious limitation of getting stuck in local optimum usually referred as premature convergence if the initially selected harmonies are in the vicinity of local optimum. In order to remove the limitations of the single metaheuristic algorithm, hybrid chaotic search/harmony search/simulated annealing algorithm is proposed, so as to increase exploration particularly in the beginning of the execution to escape local optima.

In the other words, to avoid such computational drawbacks as premature convergence, trapping in local optima, too many control parameters, and excessive sensitivity to the initial value of these parameters, we have to preserve the main control parameters of the algorithm and the diversity of new solutions during the evolution. In this regard, the combination of simulated annealing algorithm, harmony search, and chaos search algorithms can improve the solution efficiency and address the computational drawbacks. The method increases species diversity to increase the chance of attaining an optimal solution. The use of parameters of the simulated annealing and chaos search algorithms in the new solution and the decision to accept or reject it make them highly immune to being trapped in local optima and thus less vulnerable to premature convergence problems.

As a result, to provide a superior optimization tool, SA, harmony search (HS) and chaotic search (CH) are combined, leading to the hybrid chaotic search/harmony search/simulated annealing (HCHSA) algorithm. As a heuristic algorithm, HS mimics the improvisation of musicians. Since decision variables for the sizing problem are discrete integers, this problem is of the combinatorial optimization type. A discrete search technique based on harmony search (HS) is employed for efficiency. The HS method used here is that proposed in [15] as discrete HS. Several key parameters affect HS algorithm convergence: harmony memory considering rate (HMCR), which is the selection rate from the harmony memory (HM) and ranges between 0 and 1, generation bandwidth (*bw*), and pitch adjusting rate (PAR). HMCR determines whether the value of a decision variable is to be chosen from HM. Also, PAR plays a role in controlling the local search. The appropriate PAR can effectively avoid the search being trapped in a local optimum. Normally, a smaller PAR is beneficial to quickly finding the local optimal solution in the early search stage, while a larger PAR is advantageous for avoiding the local optimum in the latter stage. As a result, a dynamic change strategy for PAR is incorporated into the hybrid optimization algorithm in this study. Furthermore, the appropriate *bw* can potentially be useful in adjusting the convergence rate of the method for the optimal solution. Here, *bw* changes dynamically with generation number. With these parameters, the algorithm convergence rate can be modified to

achieve the optimal solution. The HM consists of N_h harmonies, while PAR and bw can be written as:

$$PAR(iter) = PAR_{\min} + \frac{PAR_{\max} - PAR_{\min}}{iter_{\max}} \times iter \tag{34}$$

$$bw(iter) = bw_{\max} \exp(c \cdot iter) \tag{35}$$

$$c = \frac{Ln\left(bw_{\min} / bw_{\max}\right)}{iter_{\max}} \tag{36}$$

Here, $PAR_{\min}$ and $PAR_{\max}$ denote respectively minimum and maximum pitch adjusting rates, $bw_{\max}$ and $bw_{\min}$ denote respectively the maximum and minimum bandwidths, and *iter* denotes the iteration index.

A new harmony is generated in HS with the following pseudocode [15]:

```
for k = 1:N_d
    if r_1 > HMCR
    x_new(k) = a feasible random integer number;
    else
    x_new(k) = value corresponding to a random selected harmony from HM;
    if r_2 < PAR
    x_new(k) = x_new(k) + r_w;
    end
  end
end
```

Here, N_d denotes the number of decision variables, while x_{new} denotes the improvised harmony. Also, the parameter r_w can be written as:

$$r_w = \begin{cases} 1 & r_3 < 0.5 \\ -1 & otherwise \end{cases} \tag{37}$$

Here, r_1, r_2 and r_3 are random numbers ranging from 0 to 1 and uniformly distributed.

To determine the methodology quality, the performance of the proposed hybrid algorithm is contrasted with that for the hybrid harmony search and simulated annealing (HS-SA) algorithms. A new harmony is generated in HS-SA with the following pseudocode [58]:

```
for k = 1:N_d
    if r_1 > HMCR = 0.9
    x_new(k) = a feasible random integer number;
    else
    x_new (n) = x(iter, n);
      if r_2 < PAR = 0.1
```

$x_{new}(n) = x_{new}(n) + r_w$;
end
end
end

Note that the harmony memory considering rate (*HMCR*) and pitch adjusting rate (*PAR*) are constant in the HS-SA algorithm [58].

The success of a metaheuristic method depends on the balance between exploitation and exploration. An ideal metaheuristic method must have enhanced exploitation capabilities towards the later generations and greater exploration capabilities in the earlier generations [58]. HCHSA seeks this goal. Taking inspiration from SA, the HCHSA algorithm accepts even inferior harmonies with probability determined by a parameter called temperature (T). The temperature parameter is initially kept high to favor inferior moves and hence increase the capability of escaping local optima and is linearly decreased to gradually shift the focus to exploitation of good harmonies.

For a specified area, chaotic variables can without repetition pass through each state, depending on their regularity. Chaos search (CS) is particularly applicable for this optimization area due to the dynamic and ergodic characteristics of chaotic variables. For a chaotic sequence, a logistic function is utilized in HCHSA, as per the following:

for k=1:N_d
if r_1>*HMCR*
$x_{new}(k)$ = feasible random integer by chaotic sequence;
else
$x_{new}(k) = x(iter, k)$;
if r_2<*PAR*
$x_{new}(k) = x_{new}(k) + r_w$;
end
end
end

HCHSA is same as original harmony search with the exception that even mediocre harmonies are accepted as done in simulated annealing and chaos search. In this regard, according to the pseudo code for HCHSA, HCHSA generates a new harmony as in original harmony search, based chaotic search and simulated annealing algorithms. Also, not only are the superior harmonies (compared to the worst harmony) always accepted but the inferior

harmonies are accepted with a probability determined by the fitness of the new harmony and the current temperature. The temperature parameter is gradually decreased, according to Eqs. 31 to 33, so as to reduce the probability of accepting inferior harmonies and hence to favor the exploitation of good harmonies. The flowchart of the HCHSA algorithm is shown in Fig. 2. Note that the HCHSA algorithm is the same as HS-SA, except that PAR is replaced by Eq. 34, and new harmony generated based chaotic search and simulated annealing algorithms are employed.

Fig. 2

4. Results and discussion

The goal of this work is to provide for a remote region of Kerman, Iran the electrical requirements with the proposed system for renewable energy as a stand-alone device. Wind speed and solar insolation experimental data are used for Rafsanjan, Kerman, in southern Iran (latitude: 30.40 º). Hourly mean demands over a day, based on annual means, are given in Fig. 3, while Fig. 4 illustrates an hourly breakdown of the mean wind speed over a day along with the electrical power the wind turbine correspondingly generates. Mean hourly insolation data over a day and the corresponding power produced by the PV panel is presented in Fig. 5.

Fig. 3

Fig. 4

Fig. 5

For the present renewable energy system analysis and optimization, a MATLAB code was developed. Tables 2 and 3 list model parameters used in the code for the PV collector and wind turbine, and their values.

Table 2

Table 3

As the fitness function can be characterized as non-linear and non-convex, sizing is a complex optimization task here. This task involves four decision variables: two integers (N_{H2}, and N_{BAT}) and two

continuous (A_{PV} and A_{WT}). The optimization algorithm probes the search space continuously to manage the integer decision variables; the value inserted as the fitness function is rounded. To determine the methodology quality, the performance of the proposed hybrid chaotic search/harmony search/simulated annealing (HCHSA) algorithm is contrasted with that for the simulated annealing (SA) algorithm (wf = 5; s = 0.97; T_0 = 100; $iter_{max}$ = 1000) [57] and a hybrid harmony search and simulated annealing (HS-SA) algorithm ($HMCR$ = 0.9; PAR = 0.1; T_0 = 100; s = 0.97; $iter_{max}$ = 1000) [58]. The HCHSA parameter values follow: PAR_{min} = 0.1; PAR_{max} = 1; $HMCR$ = 0.9; T_0 = 100; s = 0.97; $iter_{max}$ = 1000. The setting of $iter_{max}$ is highly problem dependent (complexity of the search space and number of variables). The maximum and minimum decision variable bounds are set to 200 and 0, respectively. The maximum number of iterations allowed in all investigated algorithms is 1000. In this study, based on the convergence process of the algorithm, $iter_{max}$ was set so that the algorithm can be able to converge to the solution. For these algorithms, the adjustable parameters are set by trial and error and finally selecting the numbers that yield best results. Because of the stochastic nature of evolutionary algorithms, each algorithm is run 50 times and the best solution of the algorithm over the runs is reported. The charge of each battery and the hydrogen tank is assumed initially to be at 30 % of its nominal capacity.

For comparing algorithm performance and for the robustness of the algorithms, 50 independent runs are conducted. Table 4 lists the statistical results, via the following indexes: Min. and Max. (minimum and maximum values respectively of fitness functions determined with the algorithm for 50 runs), Mean (mean of values of fitness function), and Std. (standard deviation value found by the SA, HS-SA, and HCHSA algorithms over 50 runs).

Table 4 shows that the minimum values for LCC for the optimized solar/wind/hydrogen, solar/hydrogen, and wind/hydrogen systems are \$19900, \$34320, and \$21320, respectively. These values are obtained with the HCHSA, SA, and HS-SA algorithms. For the solar/wind/hydrogen system, the relative error between the Mean index of SA

and HCHSA, $\left|\frac{Min_{SA}-Min_{HCHSA}}{Min_{SA}}\right|\times 100$, is 11.47%, and between the Mean index of HS-SA and HCHSA is 3.24%. For the solar/hydrogen system, the relative error between the Mean index of SA and HCHSA is 0.76%, and between the Mean index of HCHSA and HS-SA is 0.5 %. The relative error between the Mean index of HCHSA and SA is 26.05% for the wind/hydrogen system. The performance is more beneficial with HCHSA than the HS-SA and SA algorithms, respectively, for the wind/hydrogen system. For the solar/wind/hydrogen and solar/hydrogen systems, the SA algorithm is superior to the HCHSA and HS-SA algorithms based on the different indexes.

Also, it is seen that the minimum LCC values for the optimized solar/wind/battery, solar/battery, and wind/battery systems are \$4000, \$4510, and \$3750, respectively. These values are obtained with HCHSA, HS-SA, and SA algorithms. After the HCHSA algorithms, the best performance in terms of the Mean index is exhibited by HS-SA and SA, respectively. It is observed that the relative error between the Mean index of HCHSA and SA is 16.24%, and between the Mean index of HCHSA and HS-SA is 0.42%, for the solar/wind/battery system. In this system, the relative error between the Max. index of the HCHSA and SA is 10.82%, and between the Max. index of the HCHSA and HS-SA is 18.79%. Also, if the Std. index is considered, the rank of these algorithms is HCHSA, HS-SA, and SA, respectively. For the solar/battery system, the relative error between the Mean index of the HCHSA and SA is 4.64%, and between the Mean index of the HCHSA and HS-SA is 0.4%. Also the relative error between the Max. index of HCHSA and SA is 8.81%. As a result, considering the Min., Max., Mean, and Std. indexes, the best performance is achieved by the HCHSA algorithm for this system. For the wind/battery system, it can be observed that the relative error between the Mean. index of the HCHSA and the SA is 32.07%, between the Mean. index of the HCHSA and the HS-SA is 5.57%, and between the Max. index of the HCHSA and SA is 20.03%. As a result, based on various indexes, the algorithms can be listed in rank order as follows: HCHSA, HS-SA, and SA. Finally, a comparison of the Min., Max., Mean, and Std. values, for the six hybrid systems, shows that the proposed HCHSA algorithm is

more robust than the HS-SA and SA algorithms since it has lower index values.

Table 4

Table 5 lists the optimal decision variables determined by HCHSA, HS-SA, and SA algorithms for six hybrid renewable energy systems: solar/wind/hydrogen, solar/hydrogen, wind/hydrogen, solar/wind/battery, solar/battery, and wind/battery systems. These decision variables are linked with the Min. indexes of HCHSA, HS-SA, and SA algorithms during 50 runs. The optimum capacities of the hybrid systems for renewable energy are listed in Table 5 for the Min. index found by HCHSA, HS-SA, and SA algorithms. The LCC values of the solar/wind/hydrogen, wind/hydrogen and solar/hydrogen systems are obtained \$19900, \$21320 and \$34320, respectively. For solar/wind/hydrogen system, it is seen that the best LCC determined by the HCHSA is similar to that determined by HS-SA and SA algorithms. As a result, for the optimal solar/wind/hydrogen system, the value of LCC is \$19900. The portion of PV, WT, FC, electrolyzer, converter/inverter, and hydrogen tanks from this value is 0.23%, 14%, 25%, 25%, 7% and 28.77%, respectively. For the optimal solar/hydrogen system, the value of LCC is \$34320. The portion of PV, FC, electrolyzer, converter/inverter, and hydrogen tanks from this value is \$42371, \$4943, \$4943, \$777 and \$19420, respectively. The optimal design of this system is A_{PV} = 92.02 m^2 and N_{H2} = 121, while the optimal number of photovoltaic panels is found to be 86. Comparing solar/wind/hydrogen and solar/hydrogen systems shows that the solar/wind/hydrogen system is superior, with a savings of \$14420. At wind/hydrogenn system, the best value of LCC is \$21320. It can be seen that the optimal values of A_{WT} and N_{WT} is determined to be 25.12 m^2 and 8; moreover, the optimal rating of WT is seen to be 8 kW. Comparing solar/hydrogen and wind/hydrogen systems shows that the wind/hydrogen system is superior, with a savings of \$13000. Finally, among these hybrid systems for supplying electrical power, the solar/wind/hydrogen system appears to be superior economically. In this case, optimal values of A_{WT}, A_{PV}, and N_{H2} are found to be 25.12 m^2, 1.07 m^2, and 36, respectively. By considering the optimal areas for the PV collectors and wind turbines, optimal numbers of PV collectors and wind turbines are obtained as 1 and 8, respectively. Also, the

optimum ratings of these components are 8 kW and 120 W, respectively. It is observed that the optimum numbers of hydrogen tanks for the solar/hydrogen and wind/hydrogen systems respectively are 121 and 47; these values exceed the corresponding values for the solar/wind/hydrogen system. The minimum LCC values for the optimized solar/wind/battery, wind/battery, and solar/battery systems respectively are determined to be \$4000, \$3750 and \$4510. For the solar/wind/battery system, the best LCC determined by the HCHSA (\$4000) is similar to that determined by HS-SA (\$4000) and SA (\$4000). As a result, the portions of PV, WT, batteries, and converter/inverter of the value of LCC are 9%, 54%, 5%, and 32%, respectively. It can be seen that the optimal values of A_{WT} and A_{PV} are determined to be 18.84 m^2 and 7.49 m^2, respectively. Comparing the solar/wind/battery and solar/wind/hydrogen systems shows that the solar/wind/battery system is superior, with a savings of \$15900. For the solar/battery system, the best value of LCC is \$4510. It can be seen that the optimal values of A_{PV} and N_{PV} are determined to be 50.29 m^2 and 47, respectively. Comparing the solar/hydrogen and solar/battery systems shows that the solar/battery system is superior, with a savings of \$29810. Also, comparing solar/battery and solar/wind/battery systems shows that the solar/wind/battery system is superior. For the optimal wind/battery system, the value of LCC is \$3750. The portions of WT, converter/inverter, and storage system from this value are \$2498, \$1036, and \$210, respectively. Comparing wind/battery and wind/hydrogen systems shows that the wind/battery system is superior. Finally, among these systems, the wind/battery system is clearly advantageous economically for supplying power. Then, optimal values for A_{WT} and N_{BAT} are found to be 21.98 m^2 and 7, respectively. By considering the optimal swept areas of the wind turbines, the number of wind turbine units that is optimal is found to be 7. The optimum numbers of batteries for the solar/wind/battery and solar/battery systems, respectively, are determined to 7 and 47. Note that the best performances over 50 runs are observed to be the same for the HCHSA, HS-SA, and SA algorithms. Finally, note that the results obtained in this study are valid for the considered case study since the results of hybrid renewable systems are directly affected by the environmental conditions (i.e. solar radiation and wind

speed) and the component types. Designing a hybrid system in another location with other types of the components than the ones used in this study may lead to different results.

Table 5

For a better understanding of the relevant component economics for the six hybrid systems for renewable energy considered and a comprehensive comparison, breakdowns of the component costs are provided in Figs. 6 and 7. As seen in Fig. 5.a, for the solar/wind/hydrogen system, the storage system (including fuel cell, electrolyzer, and hydrogen tanks) is largest cost component, accounting for 79% of the cost of the system. It is also shown that the cost of the hydrogen tanks accounts for 29% of the cost of the storage system, and is the largest component cost. Similarly, the hydrogen tanks account for 57% of the cost for the solar/hydrogen system and 35% for the wind/hydrogen system, and are the largest component cost among the component costs of the system. Finally, the hydrogen storage system is observed to have the largest component cost among the hydrogen storage-based hybrid energy systems. Fig. 6.a-c. shows that the wind turbines in solar/wind/battery system account for 54% of the system cost, the PV system in solar/battery system account for 52%, and the wind turbines in wind/battery system account for 67% and represent the largest cost of the components of the systems. Also, it can be seen that battery storage costs vary in different situations and are one of the most effective components of hybrid systems.

Fig. 6

Fig. 7

The convergence processes for the HCHSA, HS-SA, and SA algorithms for each of the six hybrid renewable energy systems considered are shown in Figs. 8 and 9. More rapid algorithm convergence reduces computational effort. It is also shown that the applied hybrid optimization algorithm can generate a solution in a significantly shorter time than single optimization algorithms; it is also shown that the hybrid optimization algorithm has good convergence. It is seen that the objective function

converges after roughly 900 generations to the optimum value. Thus, 1000 generations are taken here to be a reasonable stopping criterion.

Fig. 8

Fig. 9

The storage levels of the battery and hydrogen storage systems are displayed in Fig. 10 on an hourly basis. The profiles for solar/wind/hydrogen and solar/wind/battery systems are similar, mainly since their loads are the same and their system generations are similar. Since the battery storage level is not allowed to drop below the minimum state of charge ($SOC_{BS\text{-}min}$), the storage levels do not go as low for the batteries as for the hydrogen tanks. Further, greater hydrogen storage is needed since the difference between the minimum and maximum storage level peaks for the solar/wind/battery system are lower than for the solar/wind/hydrogen system. This is attributable to the lower efficiency of hydrogen storage compared to battery storage.

The results suggest that the better candidate for energy storage, based on economics, is the battery. Although hydrogen energy storage systems are found here to be less economic than battery storage systems, they have other benefits: The FC/electrolyzer storage system has a small footprint and is environmentally beneficial. If in the future the efficiencies increase and costs decrease for the fuel cell and the electrolyzer, then the FC/electrolyzer storage may become more economic.

Fig. 10

5. Conclusions

To increase the cost-effectiveness and reliability of energy systems, an efficient methodology is proposed for modeling and optimally sizing a hybrid system for renewable energy (wind and solar) considering two storage device options: chemical storage via hydrogen and electrochemical storage via batteries. The hybrid systems for renewable energy are modeled, considering four decision variables: area swept by rotating blades of the wind turbine, surface area of PV collectors, and storage system capacities (battery and hydrogen tank). To solve this complex optimization problem, a modified version

is proposed of the simulated annealing algorithm-based chaotic search and harmony search algorithms. Results are compared for this algorithm and simulated annealing (SA) and hybrid harmony search and simulated annealing (HS-SA) algorithms. The proposed modified approach is used to size optimally the components of six system schemes: wind/battery, solar/battery and solar/wind/battery, as well as wind/hydrogen, solar/hydrogen, and solar/wind/hydrogen. The electric demand for a remote area in Iran is satisfied by all systems. It is concluded that on average the proposed methodology (hybrid chaotic search/harmony search/simulated annealing (HCHSA)) attains more accurate results than the other algorithms. As a result, a comparison of the Min., Max., Mean, and Std. values, in the six hybrid systems, shows that the proposed HCHSA algorithm is more robust than the HS-SA and SA algorithms since it has lower index values. It can be observed that the relative error between the Mean index of HCHSA and SA is 11.13%, and between the Mean index of HCHSA and HS-SA is 1.34%, and between the Mean index of HS-SA and SA is 9.44%. Finally, based on various indexes, the algorithms can be listed in rank order as follows: HCHSA, HS-SA, and SA. Also, it is seen through the optimization results that a solar and wind energy based hybrid system with electrochemical storage via a bench of batteries provides more reliable and cost effective energy than a hybrid system for renewable energy using chemical (hydrogen) storage. Nevertheless, the latter energy system is reliable and non-polluting and, with cost and efficiency improvements in the fuel cell and electrolyzer, the option of hydrogen storage in the future may prove economically advantageous. Finally, among the hybrid energy systems considered, the results indicate the most reliable and cost effective stand-alone system for providing the electrical demanded for a remote region in Kerman, Iran is the hybrid solar and battery system. As a result, the portions of the wind turbines, batteries, and converter/inverter comprising the value of the life cycle cost are 67%, 5%, and 28%, respectively.

References

[1] A. Maleki, "Design and optimization of autonomous solar-wind-reverse osmosis desalination systems coupling battery and hydrogen energy storage by an improved bee algorithm," *Desalination,* vol. 435, pp. 221-234, 2018.

[2] G. Kyriakarakos, A. I. Dounis, K. G. Arvanitis, and G. Papadakis, "Design of a Fuzzy Cognitive Maps variable-load energy management system for autonomous PV-reverse osmosis desalination systems: A simulation survey," *Applied Energy,* vol. 187, pp. 575-584, 2017.

[3] D. Nelson, M. Nehrir, and C. Wang, "Unit sizing and cost analysis of stand-alone hybrid wind/PV/fuel cell power generation systems," *Renewable Energy,* vol. 31, pp. 1641-1656, 2006.

[4] O. Ekren and B. Y. Ekren, "Size optimization of a PV/wind hybrid energy conversion system with battery storage using simulated annealing," *Applied Energy,* vol. 87, pp. 592-598, 2010.

[5] M. Calderón, A. Calderón, A. Ramiro, and J. González, "Automatic management of energy flows of a stand-alone renewable energy supply with hydrogen support," *International Journal of Hydrogen Energy,* vol. 35, pp. 2226-2235, 2010.

[6] T. Khatib, A. Mohamed, K. Sopian, and M. Mahmoud, "Optimal sizing of building integrated hybrid PV/diesel generator system for zero load rejection for Malaysia," *Energy and Buildings,* vol. 43, pp. 3430-3435, 2011.

[7] R. Dufo-López, J. L. Bernal-Agustín, J. M. Yusta-Loyo, J. A. Domínguez-Navarro, I. J. Ramírez-Rosado, J. Lujano*, et al.*, "Multi-objective optimization minimizing cost and life cycle emissions of stand-alone PV–wind–diesel systems with batteries storage," *Applied Energy,* vol. 88, pp. 4033-4041, 2011.

[8] R. Belfkira, L. Zhang, and G. Barakat, "Optimal sizing study of hybrid wind/PV/diesel power generation unit," *Solar Energy,* vol. 85, pp. 100-110, 2011.

[9] A. S. Raj and P. C. Ghosh, "Standalone PV-diesel system vs. PV-H2 system: An economic analysis," *Energy,* vol. 42, pp. 270-280, 2012.

[10] R. Valdés, L. Rodríguez, and J. Lucio, "Procedure for optimal design of hydrogen production plants with reserve storage and a stand-alone photovoltaic power system," *International Journal of Hydrogen Energy,* vol. 37, pp. 4018-4025, 2012.

[11] G. Merei, C. Berger, and D. U. Sauer, "Optimization of an off-grid hybrid PV–Wind–Diesel system with different battery technologies using genetic algorithm," *Solar Energy,* vol. 97, pp. 460-473, 2013.

[12] M. Castañeda, A. Cano, F. Jurado, H. Sanchez, and L. M. Fernandez, "Sizing optimization, dynamic modeling and energy management strategies of a stand-alone PV/hydrogen/battery-based hybrid system," *International Journal of Hydrogen Energy,* vol. 38, pp. 3830-3845, 2013.

[13] A. Hiendro, R. Kurnianto, M. Rajagukguk, and Y. M. Simanjuntak, "Techno-economic analysis of photovoltaic/wind hybrid system for onshore/remote area in Indonesia," *Energy,* vol. 59, pp. 652-657, 2013.

[14] D. Rekioua, S. Bensmail, and N. Bettar, "Development of hybrid photovoltaic-fuel cell system for stand-alone application," *International Journal of Hydrogen Energy,* vol. 39, pp. 1604-1611, 2014.

[15] A. Maleki and A. Askarzadeh, "Optimal sizing of a PV/wind/diesel system with battery storage for electrification to an off-grid remote region: A case study of Rafsanjan, Iran," *Sustainable Energy Technologies and Assessments,* vol. 7, pp. 147-153, 2014.

[16] S. Bensmail, D. Rekioua, and H. Azzi, "Study of hybrid photovoltaic/fuel cell system for stand-alone applications," *International Journal of Hydrogen Energy,* vol. 40, pp. 13820-13826, 2015.

[17] D. Tsuanyo, Y. Azoumah, D. Aussel, and P. Neveu, "Modeling and optimization of batteryless hybrid PV (photovoltaic)/Diesel systems for off-grid applications," *Energy,* vol. 86, pp. 152-163, 2015.

[18] A. Chauhan and R. Saini, "Discrete harmony search based size optimization of Integrated Renewable Energy System for remote rural areas of Uttarakhand state in India," *Renewable Energy,* vol. 94, pp. 587-604, 2016.

[19] G. Shankar and V. Mukherjee, "Load frequency control of an autonomous hybrid power system by quasi-oppositional harmony search algorithm," *International Journal of Electrical Power & Energy Systems,* vol. 78, pp. 715-734, 2016.

[20] L. M. Halabi, S. Mekhilef, L. Olatomiwa, and J. Hazelton, "Performance analysis of hybrid PV/diesel/battery system using HOMER: A case study Sabah, Malaysia," *Energy Conversion and Management,* vol. 144, pp. 322-339, 2017.
[21] O. Nadjemi, T. Nacer, A. Hamidat, and H. Salhi, "Optimal hybrid PV/wind energy system sizing: Application of cuckoo search algorithm for Algerian dairy farms," *Renewable and Sustainable Energy Reviews,* vol. 70, pp. 1352-1365, 2017.
[22] A. Hatata, G. Osman, and M. Aladl, "An optimization method for sizing a solar/wind/battery hybrid power system based on the artificial immune system," *Sustainable Energy Technologies and Assessments,* vol. 27, pp. 83-93, 2018.
[23] J. Ahmad, M. Imran, A. Khalid, W. Iqbal, S. R. Ashraf, M. Adnan*, et al.*, "Techno economic analysis of a wind-photovoltaic-biomass hybrid renewable energy system for rural electrification: A case study of Kallar Kahar," *Energy,* vol. 148, pp. 208-234, 2018.
[24] D. Guangqian, K. Bekhrad, P. Azarikhah, and A. Maleki, "A hybrid algorithm based optimization on modeling of grid independent biodiesel-based hybrid solar/wind systems," *Renewable Energy,* vol. 122, pp. 551-560, 2018.
[25] W. Peng, A. Maleki, M. A. Rosen, and P. Azarikhah, "Optimization of a hybrid system for solar-wind-based water desalination by reverse osmosis: Comparison of approaches," *Desalination,* vol. 442, pp. 16-31, 2018.
[26] M. Eteiba, S. Barakat, M. Samy, and W. I. Wahba, "Optimization of an Off-Grid PV/Biomass Hybrid System with Different Battery Technologies," *Sustainable Cities and Society,* vol. 40, pp. 713-727, 2018.
[27] A. Khiareddine, C. B. Salah, D. Rekioua, and M. F. Mimouni, "Sizing methodology for hybrid photovoltaic/wind/hydrogen/battery integrated to energy management strategy for pumping system," *Energy,* vol. 153, pp. 743-762, 2018.
[28] E. Koutroulis, D. Kolokotsa, A. Potirakis, and K. Kalaitzakis, "Methodology for optimal sizing of stand-alone photovoltaic/wind-generator systems using genetic algorithms," *Solar Energy,* vol. 80, pp. 1072-1088, 2006.
[29] M. Ismail, M. Moghavvemi, and T. Mahlia, "Techno-economic analysis of an optimized photovoltaic and diesel generator hybrid power system for remote houses in a tropical climate," *Energy Conversion and Management,* vol. 69, pp. 163-173, 2013.
[30] W. Chong, M. Naghavi, S. Poh, T. Mahlia, and K. Pan, "Techno-economic analysis of a wind–solar hybrid renewable energy system with rainwater collection feature for urban high-rise application," *Applied Energy,* vol. 88, pp. 4067-4077, 2011.
[31] G. Tzamalis, E. Zoulias, E. Stamatakis, E. Varkaraki, E. Lois, and F. Zannikos, "Techno-economic analysis of an autonomous power system integrating hydrogen technology as energy storage medium," *Renewable Energy,* vol. 36, pp. 118-124, 2011.
[32] K. Karakoulidis, K. Mavridis, D. Bandekas, P. Adoniadis, C. Potolias, and N. Vordos, "Techno-economic analysis of a stand-alone hybrid photovoltaic-diesel–battery-fuel cell power system," *Renewable Energy,* vol. 36, pp. 2238-2244, 2011.
[33] A. Kaabeche, M. Belhamel, and R. Ibtiouen, "Sizing optimization of grid-independent hybrid photovoltaic/wind power generation system," *Energy,* vol. 36, pp. 1214-1222, 2011.
[34] A. Kaabeche and R. Ibtiouen, "Techno-economic optimization of hybrid photovoltaic/wind/diesel/battery generation in a stand-alone power system," *Solar Energy,* vol. 103, pp. 171-182, 2014.
[35] F. Caballero, E. Sauma, and F. Yanine, "Business optimal design of a grid-connected hybrid PV (photovoltaic)-wind energy system without energy storage for an Easter Island's block," *Energy,* vol. 61, pp. 248-261, 2013.
[36] S. Rajanna and R. Saini, "Development of optimal integrated renewable energy model with battery storage for a remote Indian area," *Energy,* vol. 111, pp. 803-817, 2016.

[37] A. Fathy, "A reliable methodology based on mine blast optimization algorithm for optimal sizing of hybrid PV-wind-FC system for remote area in Egypt," *Renewable Energy,* vol. 95, pp. 367-380, 2016.
[38] A. Hassan, M. Saadawi, M. Kandil, and M. Saeed, "Modified particle swarm optimisation technique for optimal design of small renewable energy system supplying a specific load at Mansoura University," *IET Renewable Power Generation,* vol. 9, pp. 474-483, 2015.
[39] P. Suhane, S. Rangnekar, A. Mittal, and A. Khare, "Sizing and performance analysis of standalone wind-photovoltaic based hybrid energy system using ant colony optimisation," *IET Renewable Power Generation,* vol. 10, pp. 964-972, 2016.
[40] S. Mishra, C. Panigrahi, and D. Kothari, "Design and simulation of a solar–wind–biogas hybrid system architecture using HOMER in India," *International Journal of Ambient Energy,* vol. 37, pp. 184-191, 2016.
[41] N. Ghorbani, A. Kasaeian, A. Toopshekan, L. Bahrami, and A. Maghami, "Optimizing a Hybrid Wind-PV-Battery System Using GA-PSO and MOPSO for Reducing Cost and Increasing Reliability," *Energy,* vol. 154, pp. 581-591, 2017.
[42] S. S. Singh and E. Fernandez, "Modeling, size optimization and sensitivity analysis of a remote hybrid renewable energy system," *Energy,* vol. 143, pp. 719-731, 2018.
[43] M. Tahani, N. Babayan, and A. Pouyaei, "Optimization of PV/Wind/Battery stand-alone system, using hybrid FPA/SA algorithm and CFD simulation, case study: Tehran," *Energy Conversion and Management,* vol. 106, pp. 644-659, 2015.
[44] R. Kumar, R. Gupta, and A. K. Bansal, "Economic analysis and power management of a stand-alone wind/photovoltaic hybrid energy system using biogeography based optimization algorithm," *Swarm and Evolutionary Computation,* vol. 8, pp. 33-43, 2013.
[45] S. Ahmadi and S. Abdi, "Application of the Hybrid Big Bang–Big Crunch algorithm for optimal sizing of a stand-alone hybrid PV/wind/battery system," *Solar Energy,* vol. 134, pp. 366-374, 2016.
[46] S. Sinha and S. Chandel, "Review of recent trends in optimization techniques for solar photovoltaic–wind based hybrid energy systems," *Renewable and Sustainable Energy Reviews,* vol. 50, pp. 755-769, 2015.
[47] R. Velik and P. Nicolay, "Energy management in storage-augmented, grid-connected prosumer buildings and neighborhoods using a modified simulated annealing optimization," *Computers & Operations Research,* vol. 66, pp. 248-257, 2016.
[48] A. Crossland, D. Jones, and N. Wade, "Planning the location and rating of distributed energy storage in LV networks using a genetic algorithm with simulated annealing," *International Journal of Electrical Power & Energy Systems,* vol. 59, pp. 103-110, 2014.
[49] T. Sousa, T. Soares, H. Morais, R. Castro, and Z. Vale, "Simulated annealing to handle energy and ancillary services joint management considering electric vehicles," *Electric Power Systems Research,* vol. 136, pp. 383-397, 2016.
[50] R. Velik and P. Nicolay, "Grid-price-dependent energy management in microgrids using a modified simulated annealing triple-optimizer," *Applied Energy,* vol. 130, pp. 384-395, 2014.
[51] S. Kayalvizhi, "Optimal planning of active distribution networks with hybrid distributed energy resources using grid-based multi-objective harmony search algorithm," *Applied Soft Computing,* vol. 67, pp. 387-398, 2018.
[52] G. A. Ezhilarasi and K. Swarup, "Network partitioning using harmony search and equivalencing for distributed computing," *Journal of Parallel and Distributed Computing,* vol. 72, pp. 936-943, 2012.
[53] Z. W. Geem and Y. Yoon, "Harmony search optimization of renewable energy charging with energy storage system," *International Journal of Electrical Power & Energy Systems,* vol. 86, pp. 120-126, 2017.

[54] A. Sadollah, H. Sayyaadi, D. G. Yoo, H. M. Lee, and J. H. Kim, "Mine blast harmony search: A new hybrid optimization method for improving exploration and exploitation capabilities," *Applied Soft Computing,* vol. 68, pp. 548-564, 2018.

[55] Y. Katsigiannis, P. S. Georgilakis, and E. S. Karapidakis, "Hybrid simulated annealing–tabu search method for optimal sizing of autonomous power systems with renewables," *IEEE Transactions on Sustainable Energy,* vol. 3, pp. 330-338, 2012.

[56] A. Rastgou, J. Moshtagh, and S. Bahramara, "Improved harmony search algorithm for electrical distribution network expansion planning in the presence of distributed generators," *Energy,* vol. 151, pp. 178-202, 2018.

[57] A. Maleki, "Modeling and optimum design of an off-grid PV/WT/FC/diesel hybrid system considering different fuel prices," *International Journal of Low-Carbon Technologies,* vol. 13, pp. 140-147, 2018.

[58] A. Assad and K. Deep, "A Hybrid Harmony search and Simulated Annealing algorithm for continuous optimization," *Information Sciences,* vol. 450, pp. 246-266, 2018.

[59] A. Maleki and A. Askarzadeh, "Artificial bee swarm optimization for optimum sizing of a stand-alone PV/WT/FC hybrid system considering LPSP concept," *Solar Energy,* vol. 107, pp. 227-235, 2014.

[60] A. Maleki and M. A. Rosen, "Design of a cost-effective on-grid hybrid wind–hydrogen based CHP system using a modified heuristic approach," *International Journal of Hydrogen Energy,* vol. 42, pp. 15973-15989, 2017.

[61] A. Maleki and A. Askarzadeh, "Comparative study of artificial intelligence techniques for sizing of a hydrogen-based stand-alone photovoltaic/wind hybrid system," *International Journal of Hydrogen Energy,* vol. 39, pp. 9973-9984, 2014.

[62] A. Maleki, F. Pourfayaz, H. Hafeznia, and M. A. Rosen, "A novel framework for optimal photovoltaic size and location in remote areas using a hybrid method: A case study of eastern Iran," *Energy Conversion and Management,* vol. 153, pp. 129-143, 2017.

[63] M. Khan and M. Iqbal, "Pre-feasibility study of stand-alone hybrid energy systems for applications in Newfoundland," *Renewable Energy,* vol. 30, pp. 835-854, 2005.

724 Fig. 1. Proposed hybrid system for renewable energy.

725 Fig. 2: Flowchart of HCHSA algorithm used in this study.

726 Fig. 3. Mean hourly load demand.

727 Fig. 4. Mean hourly profiles for wind speed and power generated by wind generator.

728 Fig. 5. Mean hourly profiles of insolation and power produced by PV system.

729 Fig. 6. Breakdown of LCC for hybrid energy systems with hydrogen storage. (a) solar/wind/hydrogen;

730 (b) solar/hydrogen; and (c) wind/hydrogen.

731 Fig. 7. Breakdown of the LCC for hybrid energy systems with battery storage. (a) solar/wind/battery;

732 (b) solar/battery; and (c) wind/battery.

733 Fig. 8. Convergence progress of algorithms in determining optimum size of hybrid system with

734 hydrogen storage

735 Fig. 9. Convergence progress of algorithms in determining optimum size of hybrid system with battery

736 storage.

737 Fig. 10. Storage levels. (a) Hydrogen tanks; and (b) batteries.

739 Table 1: Summary of the literature review.

740 Table 2: Wind turbine and PV panel parameters and their values.

741 Table 3: Parameters used in case study and values

742 Table 4: Results obtained by HCHSA, SA, and HS-SA algorithms for hybrid systems for renewable

743 energy.

744 Table 5: Summary of results for the algorithms.

745

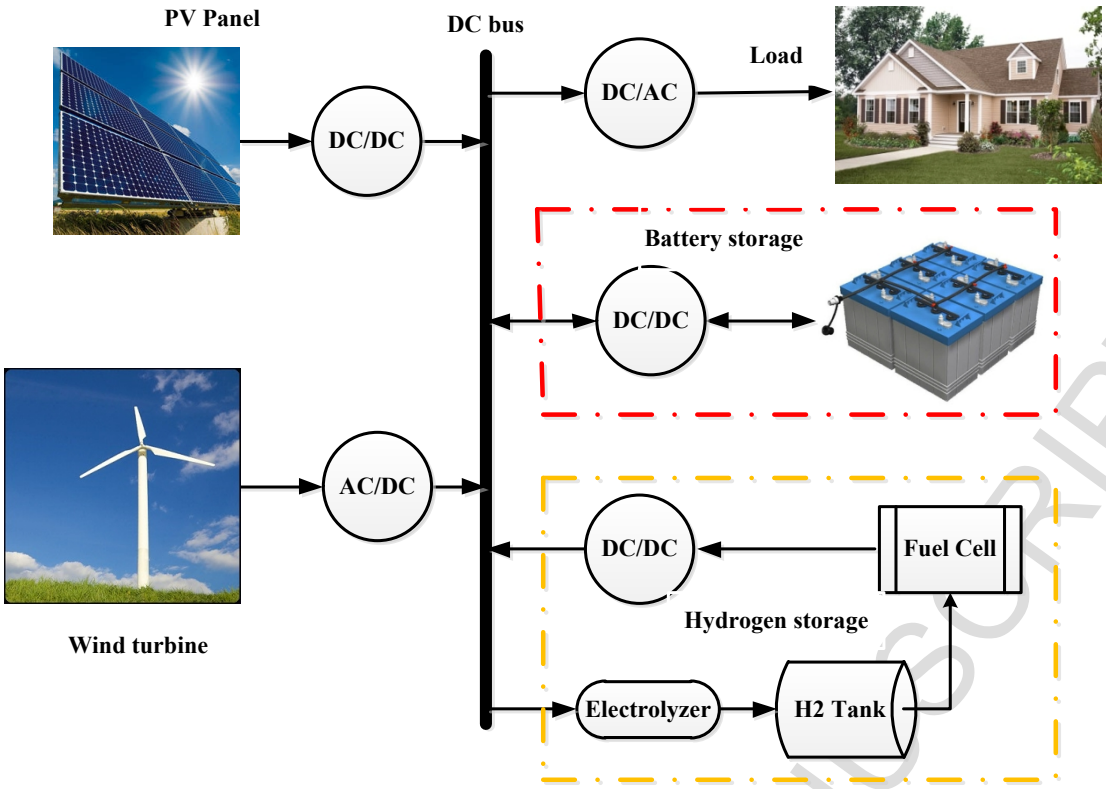

Fig. 1. Proposed hybrid system for renewable energy.

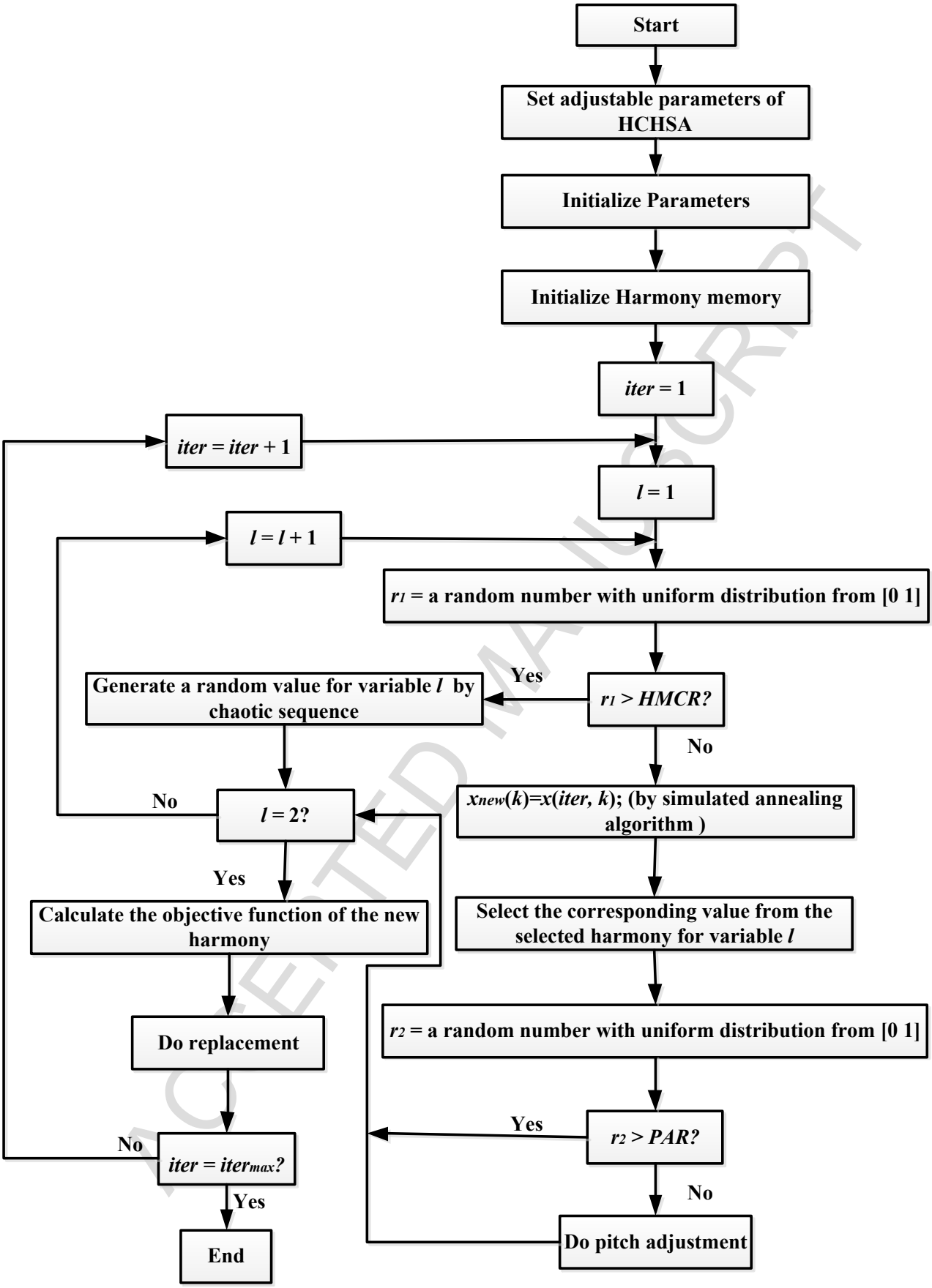

Fig. 2: Flowchart of HCHSA algorithm used in this study.

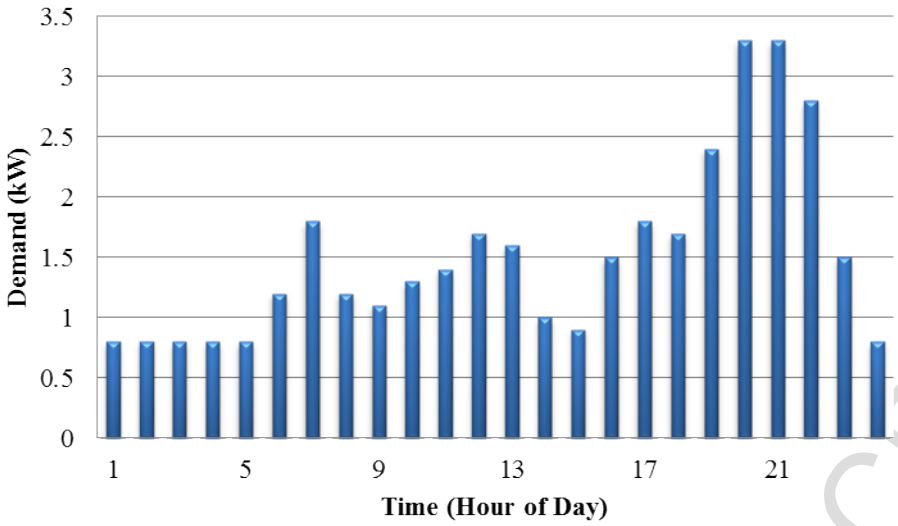

Fig. 3. Mean hourly load demand.

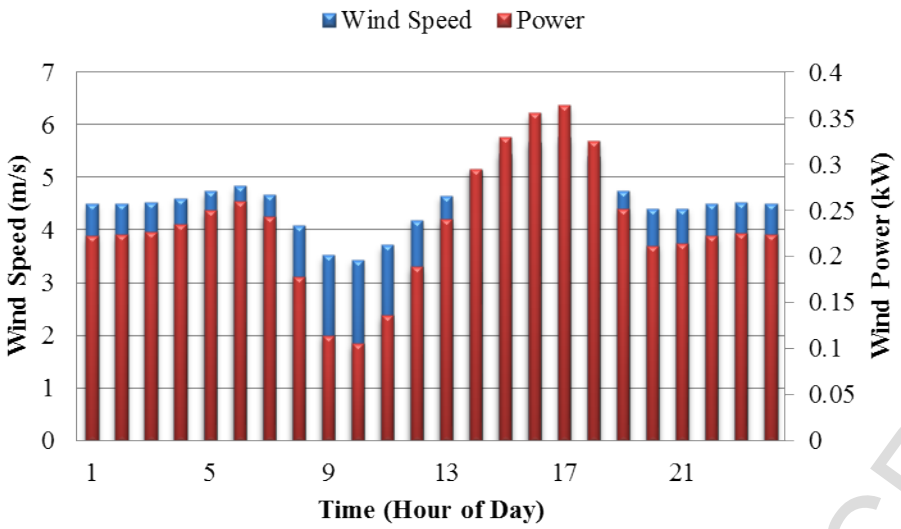

Fig. 4. Mean hourly profiles for wind speed and power generated by wind generator.

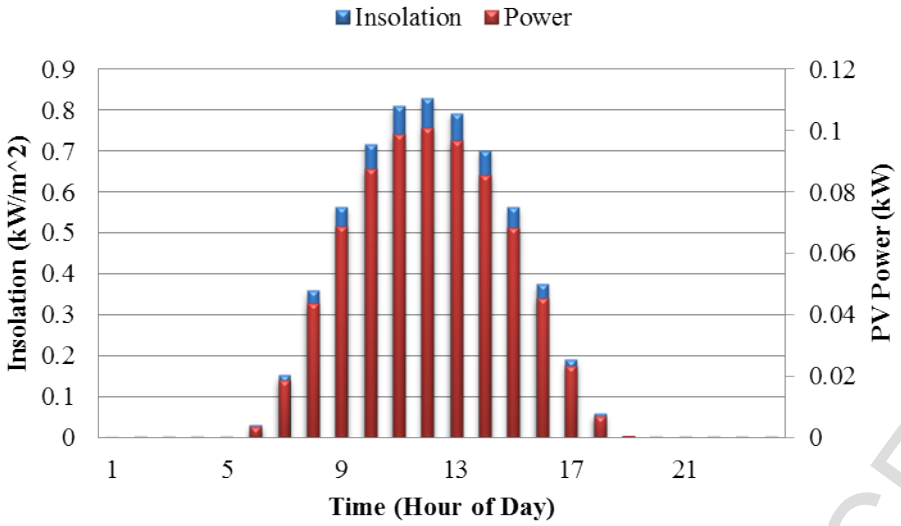

Fig. 5. Mean hourly profiles of insolation and power produced by PV system.

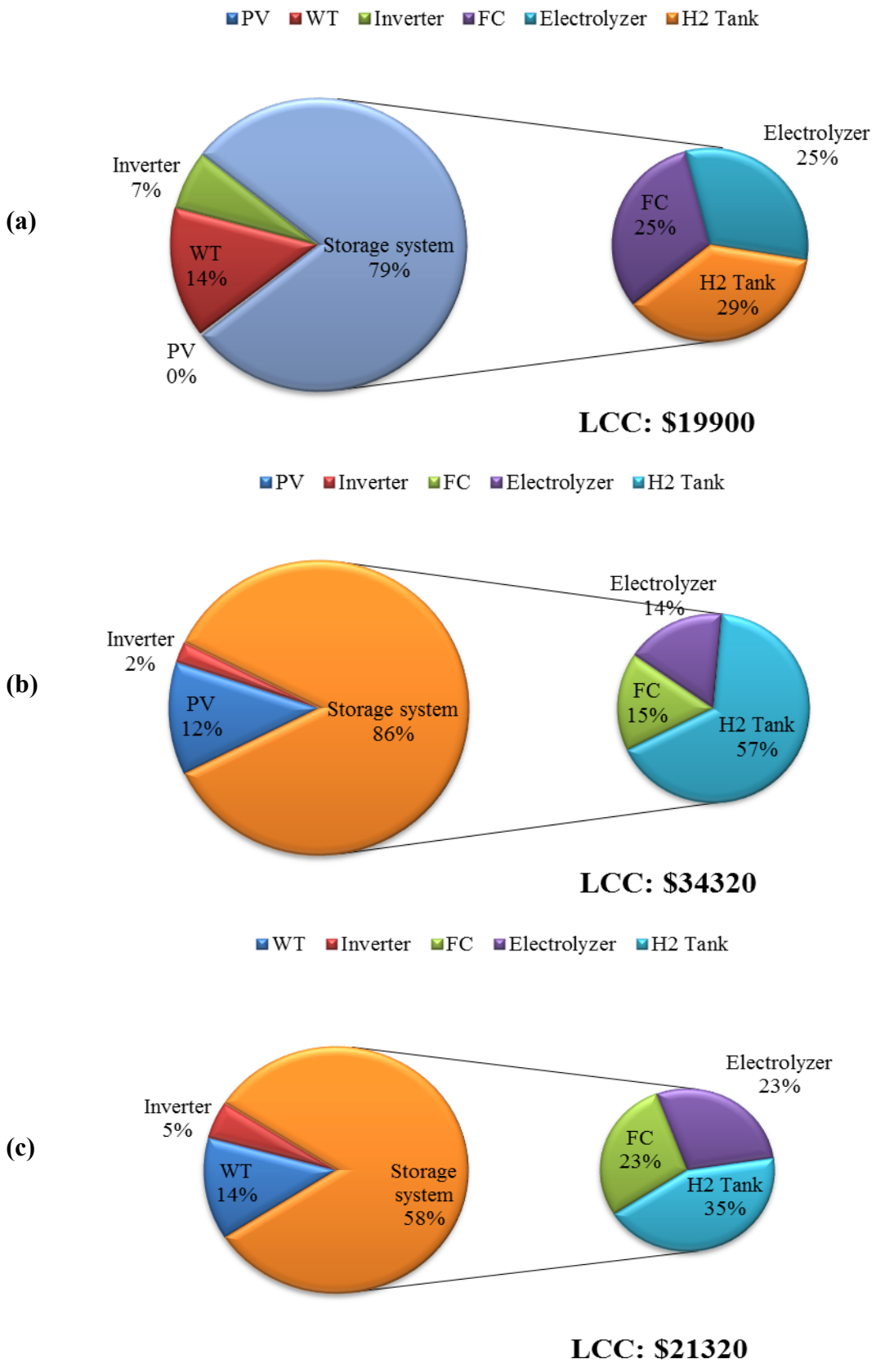

Fig. 6. Breakdown of LCC for hybrid energy systems with hydrogen storage. (a) solar/wind/hydrogen; (b) solar/hydrogen; and (c) wind/hydrogen.

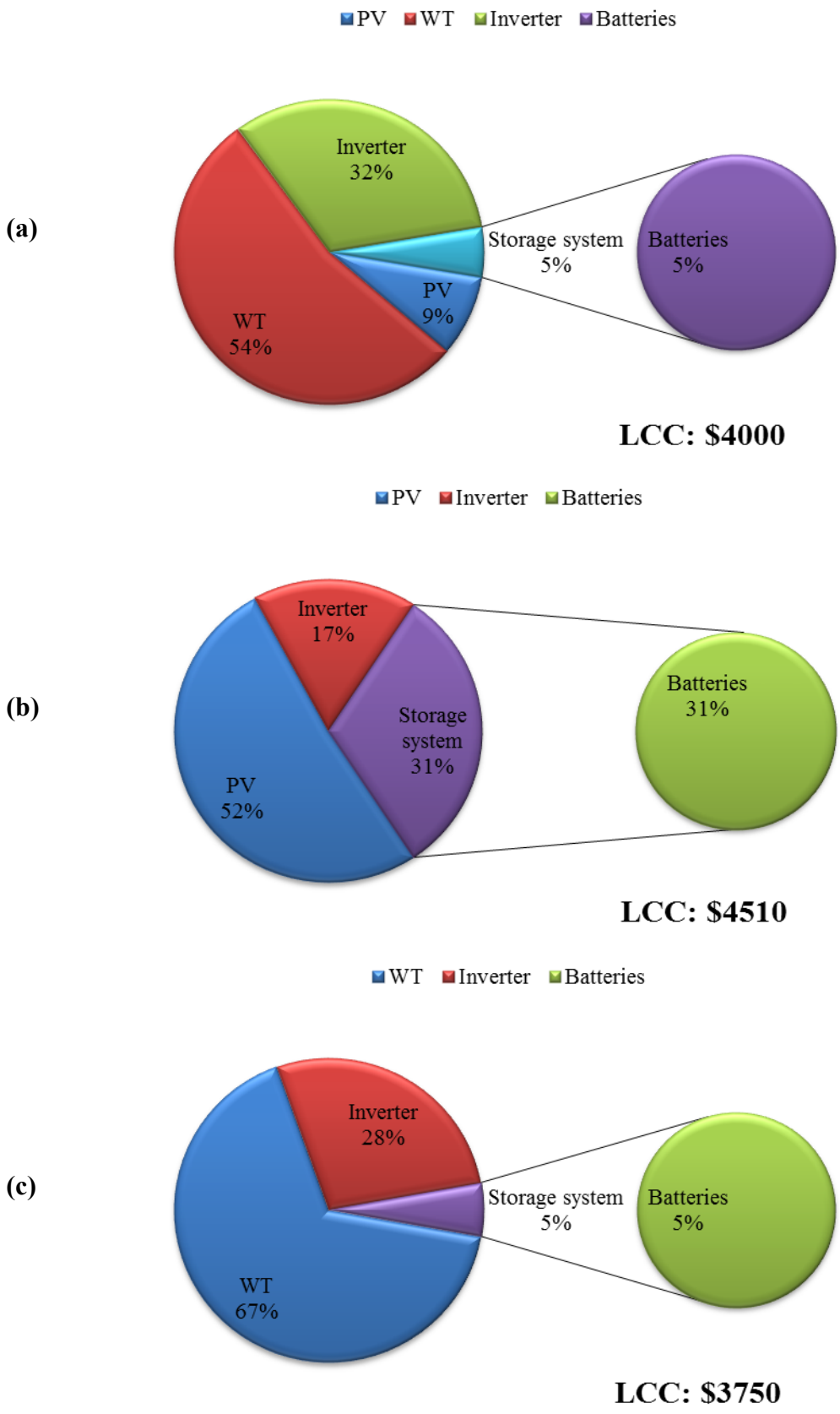

Fig. 7. Breakdown of the LCC for hybrid energy systems with battery storage. (a) solar/wind/battery; (b) solar/battery; and (c) wind/battery.

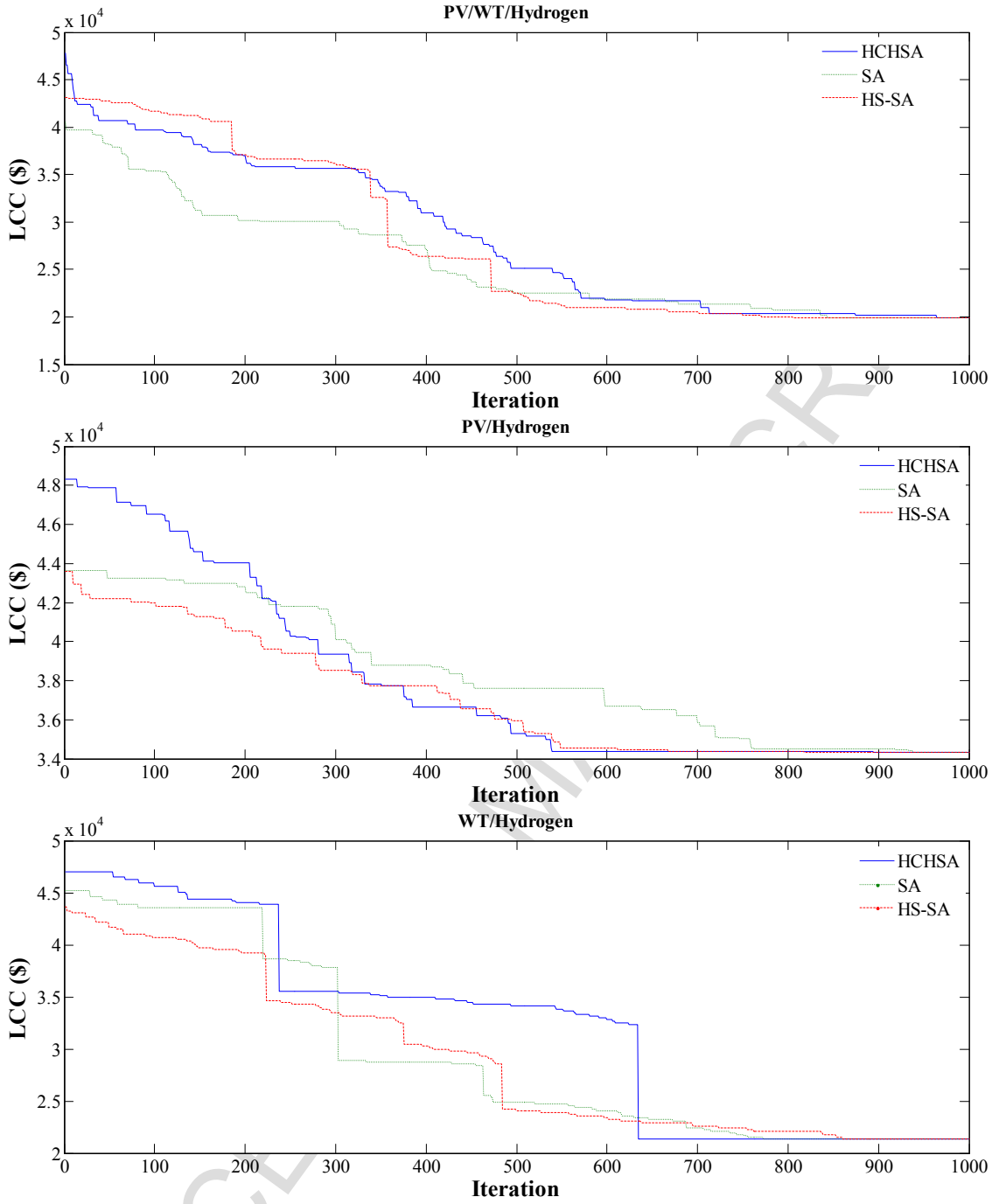

Fig. 8. Convergence progress of algorithms in determining optimum size of hybrid system with hydrogen storage

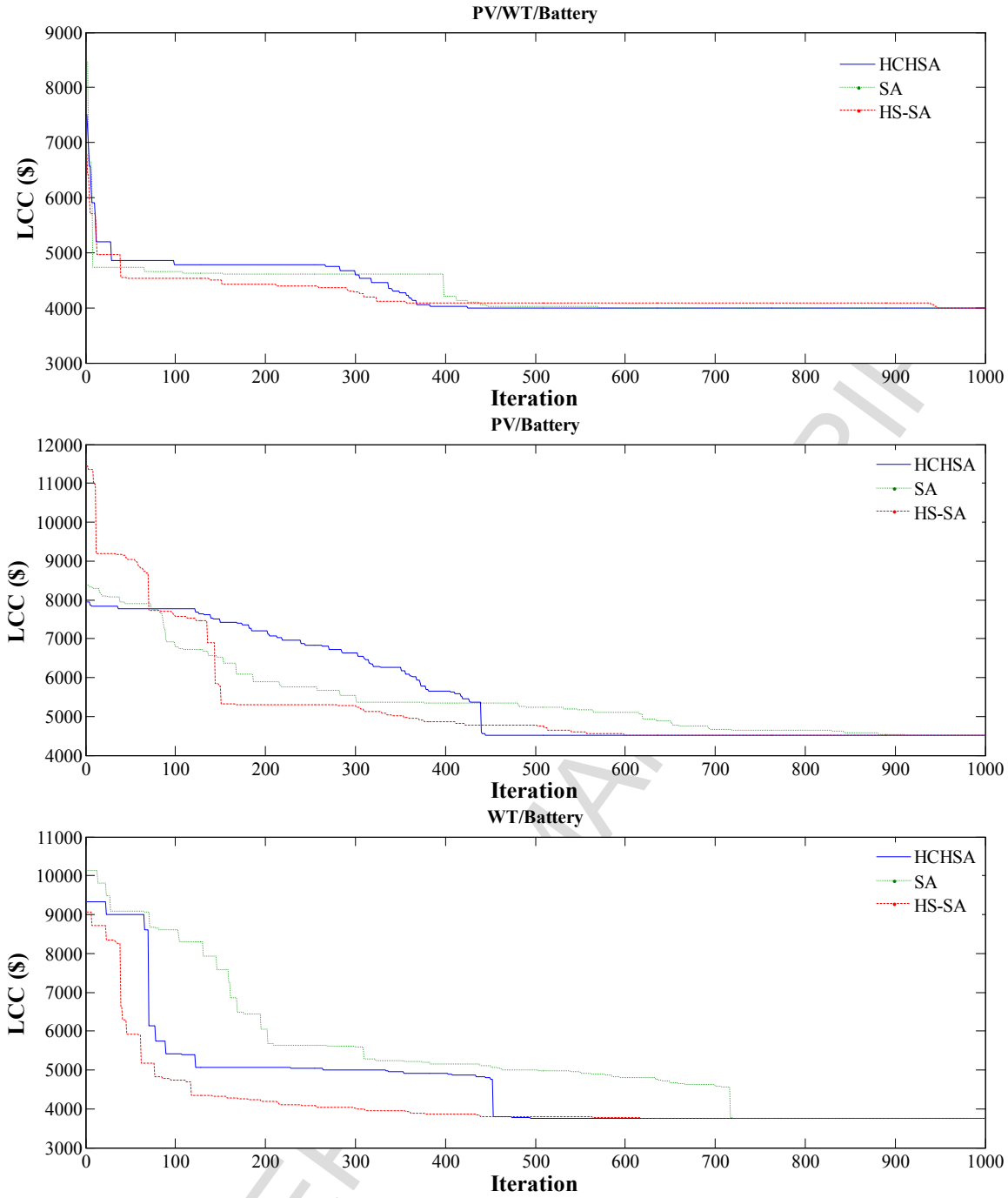

Fig. 9. Convergence progress of algorithms in determining optimum size of hybrid system with battery storage.

(a)

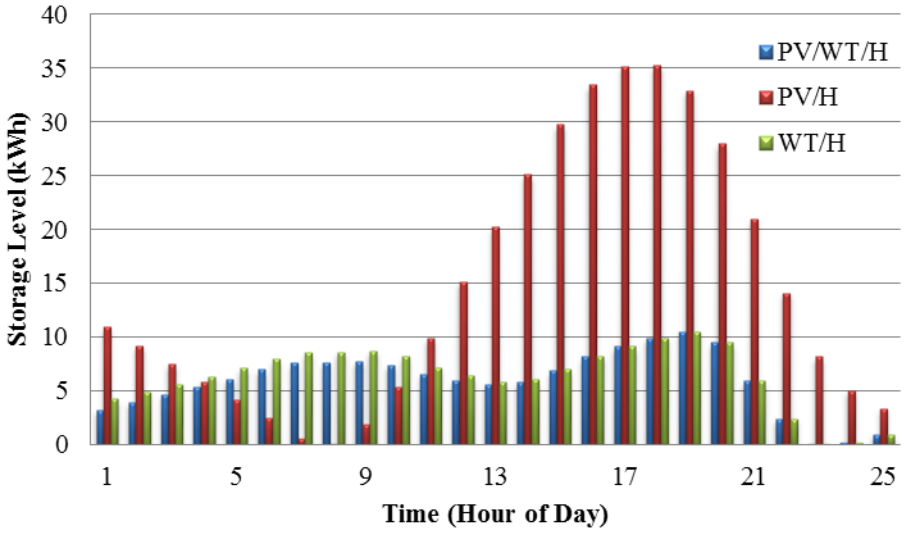

(b)

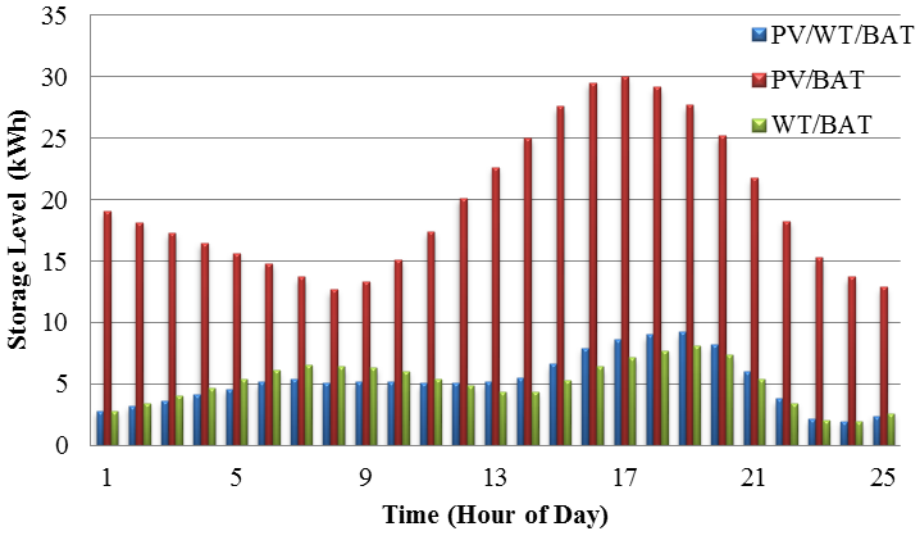

Fig. 10. Storage levels. (a) Hydrogen tanks; and (b) batteries.

Highlights

- A method is developed for optimally sizing a wind and solar energy system including battery and hydrogen storage
- Modified versions of the simulated annealing algorithm are developed
- Six hybrid systems for renewable energy that supply a remote electrical load are modeled.
- Results are analyzed and a breakdown of the life cycle cost is given.
- The hybrid chaotic search/harmony search/simulated annealing algorithm is useful for size optimization.

Table 2: Wind turbine and PV panel parameters and their values.

Wind turbine		**PV panel**	
Parameter	**Value**	**Parameter**	**Value**
P_r	1 kW	P_r	120 W
$v_{cut\text{-}in}$	2.5 m/s	C_{PV}	573.8 \$/m^2
$v_{cut\text{-}out}$	13 m/s	$C_{Mnt\text{-}PV}$	0.03 × C_{PV} \$/m^2/year
v_r	11 m/s	Life span	20 years
Life span	20 years	η_{PV}	12%
C_{WT}	1019 \$/m^2		
$C_{Mnt\text{-}WT}$	0.1×C_{WT} \$/m^2/yea		

Table 3: Parameters used in case study and values

Parameter	**Value**
j	5%
n	20 years
Fuel cell	
Rated power	3 kW
η_{FC}	50%
Life span	5 years
C_{FC}	$20000
$C_{Mtn\text{-}FC}$	1400 $/year
Electrolyzer	
Rated power	3 kW
η_{Elect}	74%
Life span	5 years
C_{Elect}	$20000
$C_{Mtn\text{-}Elec}$	1400$/year
C_{H2}	$2000
Nominal capacity of hydrogen tank	0.3 kWh
Life span of hydrogen tank	20 years
Power converter/inverter	
Rated power	3 kW
η_{inv}	95%
Life span	10 years
$C_{Conv/Inv}$	2000 $
Battery	
Voltage	12 V
C_B	1.35 kWh
η_{BC}	85 %
η_{BD}	100 %
C_{BS}	$130
Life span	5 years
DOD	0.8
σ	0.0002

Table 4: Results obtained by HCHSA, SA, and HS-SA algorithms for hybrid systems for renewable energy.

Hybrid system	**Algorithm**	**Index**				
		Mean	*Std.*	*Min.*	*Max*	*Rank*
Solar/wind/hydrogen	HCHSA	24200	3550	19900	30600	3
	SA	21710	3140	19900	30600	1
	HS-SA	23440	3460	19900	33400	2
Solar/hydrogen	HCHSA	34590	654	34320	38800	2
	SA	34330	22	34320	34500	1
	HS-SA	34760	829	34320	38800	3
Wind/hydrogen	HCHSA	22650	3062	21320	31400	1
	SA	28550	5390	21320	40100	3
	HS-SA	23640	3410	21320	32900	2
Solar/wind/battery	HCHSA	4740	607	4000	6280	1
	SA	5510	818	4000	6960	3
	HS-SA	4760	758	4000	7460	2
Solar/battery	HCHSA	4960	557	4510	6810	1
	SA	5190	661	4510	7410	3
	HS-SA	4980	564	4510	6900	2
Wind/battery	HCHSA	4490	637	3750	6040	1
	SA	5930	879	3750	7250	3
	HS-SA	4740	684	3750	6360	2
Average rank	HCHSA	1.5		Final rank	HCHSA	1
	SA	2.33			SA	3
	HS-SA	2.17			HS-SA	2

Table 5 Summary of results for the algorithms.

Solar/wind/hydrogen-based hybrid system

Algorithm	A_{PV} (m^2)	A_{WT} (m^2)	N_{PV}	N_{H2}	N_{WT}	WT cost ($)	PV cost ($)	FC cost ($)	Electrolyser cost ($)	H_2 tank cost ($)	Converter/inverter cost ($)	LCC ($)
HCHSA	1.07	25.12	1	36	8	2854	50	4943	4943	5778	1295	19900
SA	1.07	25.12	1	36	8	2854	50	4943	4943	5778	1295	19900
HS-SA	1.07	25.12	1	36	8	2854	50	4943	4943	5778	1295	19900

Solar/hydrogen -based hybrid system

Algorithm	A_{PV} (m^2)	N_{PV}	N_{H2}	PV cost ($)	FC cost ($)	Electrolyser cost ($)	H_2 tank cost ($)	Converter/inverter cost ($)	LCC ($)
HCHSA	92.02	86	121	4237	4943	4943	19420	777	34320
SA	92.02	86	121	4237	4943	4943	19420	777	34320
HS-SA	92.02	86	121	4237	4943	4943	19420	777	34320

Wind/hydrogen -based hybrid system

Algorithm	A_{WT} (m^2)	N_{WT}	N_{H2}	WT cost ($)	FC cost ($)	Electrolyser cost ($)	H_2 tank cost ($)	Converter/inverter cost ($)	LCC ($)
HCHSA	25.12	8	47	2854	4943	4943	7543	1036	21320
SA	25.12	8	47	2854	4943	4943	7543	1036	21320
HS-SA	25.12	8	47	2854	4943	4943	7543	1036	21320

Solar/wind/battery-based hybrid system

Algorithm	A_{PV} (m^2)	A_{WT} (m^2)	N_{PV}	N_{WT}	N_{BAT}	PV cost ($)	WT cost ($)	Battery cost ($)	Converter/inverter cost ($)	LCC ($)
HCHSA	7.49	18.84	7	6	7	345	2141	210	1295	4000
SA	7.49	18.84	7	6	7	345	2141	210	1295	4000
HS-SA	7.49	18.84	7	6	7	345	2141	210	1295	4000

Solar/battery-based hybrid system

Algorithm	A_{PV}(m^2)	N_{PV}	N_{BAT}	PV cost ($)	Battery cost ($)	Converter/inverter cost ($)	LCC ($)
HCHSA	50.29	47	47	2316	1412	777	4510
SA	50.29	47	47	2316	1412	777	4510
HS-SA	50.29	47	47	2316	1412	777	4510

Wind/battery-based hybrid system

Algorithm	A_{WT}(m^2)	N_{WT}	N_{BAT}	WT cost ($)	Battery cost ($)	Converter/inverter cost ($)	LCC ($)
HCHSA	21.98	7	7	2498	210	1036	3750
SA	21.98	7	7	2498	210	1036	3750
HS-SA	21.98	7	7	2498	210	1036	3750